Hindawi
International Journal of Corrosion
Volume 2018, Article ID 7345346, 24 pages
https://doi.org/10.1155/2018/7345346

Review Article

Tribocorrosion of Passive Materials: A Review on Test Procedures and Standards

A. López-Ortega,[1] **J. L. Arana**,[2] **and R. Bayón**[1]

[1]*IK4-TEKNIKER, Eibar, Spain*
[2]*Department of Metallurgical and Materials Engineering, University of the Basque Country, Spain*

Correspondence should be addressed to A. López-Ortega; ainara.lopez@tekniker.es

Received 31 January 2018; Accepted 29 April 2018; Published 7 June 2018

Academic Editor: Ramesh Chinnakurli

This paper reviews the most recent available literature relating to the electrochemical techniques and test procedures employed to assess tribocorrosion behaviour of passive materials. Over the last few decades, interest in tribocorrosion studies has notably increased, and several electrochemical techniques have been adapted to be applied on tribocorrosion research. Until 2016, the only existing standard to study tribocorrosion and to determine the synergism between wear and corrosion was the ASTM G119. In 2016, the UNE 112086 standard was developed, based on a test protocol suggested by several authors to address the drawbacks of the ASTM G119 standard. Current knowledge on tribocorrosion has been acquired by combining different electrochemical techniques. This work compiles different test procedures and a combination of electrochemical techniques used by noteworthy researchers to assess tribocorrosion behaviour of passive materials. A brief insight is also provided into the electrochemical techniques and studies made by tribocorrosion researchers.

1. Introduction

In accordance with the ASTM G 40 Standard [1], tribocorrosion can be defined as a synergetic process involving the simultaneous action of contact between surfaces in relative motion with the chemical reactions in the environment, where each process is affected by the action of the other and, in many cases, accelerated.

The first steps in the field of tribocorrosion date back to 1875, when Edison observed alterations in the coefficient of friction with different applied potentials [2]. The effect of surface chemistry on the mechanical response of materials has been investigated since the beginning of the twentieth century [3]. Between the late 1970s and early 1980s, the effect of wear on corrosion was studied by several researchers in different industrial application systems, i.e., abrasion-corrosion, erosion-corrosion, or sliding-corrosion [4]. But it was not until the 1990s that tribocorrosion mechanisms in sliding contact were proposed by Mischler et al. (1993) [5] and Madsen (1994) in a standard form [6].

Tribocorrosion encompasses several industrial sectors, e.g., material processing, energy conversion, transportation, oil and gas exploration, medical and dental implants, surgical devices, among others [2, 7, 8]. Due to its impact on daily life and potential economic benefits, interest in the study of tribocorrosion phenomenon has increased over the last few decades [3, 9, 10]. As a consequence, several electrochemical techniques have been adapted to be applied to tribocorrosion research. Thus, crucial improvements in the study of tribocorrosion have been achieved through a better interpretation of triboelectrochemical results [7, 11].

Despite growing interest and the enhancement of electrochemical techniques, standardized testing methodology for tribocorrosion evaluation has only been made available recently. Prior to 2016, the only existing standard was the ASTM G119 [6], which describes a method to determine the synergism between wear and corrosion. However, this standard has drawn criticism from several authors who developed different approaches to study the tribocorrosion behaviour of passive materials [3, 12, 13]. In 2016, a new standard (UNE 112086 [14]) was published, with a different

test protocol to address the drawbacks of the older standard. The ASTM standard involves wear testing under anodic and cathodic polarization, whereas the new standard approach involves wear tests at open circuit potential.

Up to now, knowledge acquired on tribocorrosion has been achieved by performing and combining different electrochemical techniques before, during, and after the wear process, to evaluate the influence of wear on corrosion, and vice versa. This work has compiled the combination of electrochemical techniques used by noteworthy researchers to assess tribocorrosion behaviour of passive materials and coatings in sliding contacts and divided them into different test procedures.

2. Tribocorrosion: Description and Background

2.1. Tribocorrosion. Tribocorrosion can be defined as the irreversible transformation of materials resulting from the simultaneous action of mechanical loading (e.g., friction, erosion, abrasion) and chemical/electrochemical interactions with the surrounding environment, i.e., corrosion attack. In other words, it is the interaction of chemical, electrochemical, and tribological factors in materials in mechanical contact with each other, under relative motion in a corrosive environment. It combines two major scientific areas, i.e., tribology and corrosion. The former comprises the study of friction, wear, and lubrication, whereas the latter is related to the chemical aspects of material degradation [2–5, 7, 8, 10–13, 15, 16].

Tribocorrosion involves a synergism between wear and corrosion, since the degradation caused by the combined action of mechanical and electrochemical processes is larger than the sum of each of them acting separately [2–8, 10–13, 15, 16]. This synergism can be either beneficial or detrimental, depending on the surface reactions that take place in the tribological contact [2, 7]. The reaction products formed on the surface can protect the surface by forming self-lubricating layers, or accelerating the material degradation by third-body effect, for instance [2, 7–9, 17–20].

Degradation of material due to tribocorrosion may occur under a variety of wear mechanisms (erosion, abrasion, microabrasion, fatigue, fretting, sliding wear, etc.) interacting with corrosion. Furthermore, contacts between surfaces in tribocorrosion can be both two-body or three-body contacts, and there are different contact modes such as sliding, fretting, rolling, impact, etc. The relative motion between surfaces can be either unidirectional or reciprocating [2, 3, 7, 8, 10, 16].

2.2. Tribocorrosion Test Apparatus. For tribocorrosion, the test equipment shall allow monitoring and control of both mechanical and electrochemical parameters. The apparatus used to measure tribological properties is named tribometer. A tribometer creates relative motion, either unidirectional (rotatory) or bidirectional (reciprocating), rubbing two surfaces against each other. On the other hand, electrochemical cells are used to record and control the electrochemical parameters. These cells are usually composed of three electrodes: a reference electrode, a counterelectrode, and the working electrode. The reference electrode has a stable, well-defined potential, and it is used to register the potential of the working electrode, i.e., the test sample. Typical reference electrodes are Saturated Camomel Electrodes (SCE) and Silver/Silver Chloride electrodes (Ag/AgCl). The counterelectrode is used to measure or control the current and is usually made of inert materials such as platinum, gold, or graphite. The electrodes are connected to a potentiostat to register the potential between the reference electrode and the working electrode, or the current between the counterelectrode and the working electrode. A typical tribocorrosion test setup is schematically shown in Figure 1, for a unidirectional tribometer under a ball-on-disc configuration.

There is no standardized test apparatus for tribocorrosion tests, which makes the interlaboratory comparability difficult for results [2]. Generally, existing tribometers are modified to incorporate the electrochemical cell. The electrochemical cells and all parts of the tribometer in contact with the sample or the test solution, e.g., the counter-body holder, are usually made of insulating materials such as nylon or Teflon, to provide adequate insulation for current leakages. Furthermore, the electrochemical cell must be designed so as to avoid any electrolyte leakage.

Finally, the test conditions should be selected to be as close to real conditions as possible. The contact geometry determines the contact area, and some factors such as the normal load and the sliding velocity are critical aspects, since they determine the depassivation rate of the system [7].

2.3. Historical Background. The earliest studies in the passivation phenomenon were performed using acidic solutions (e.g., sulphuric acid), and they were focused on understanding the formation of the passive film and its behaviour under corrosion-wear solicitations [16, 21–23]. The electrolyte and materials used in tribocorrosion tests were reasonably well-adapted to the technological interests, so saline solutions began to be used more in order to reproduce industrial applications [24–28] and thus predict the useful life of components more accurately. Remarkable developments in the marine industry have also promoted tribocorrosion studies in synthetic seawater in later years [29–34]. On the other hand, developing coatings with enhanced wear and corrosion properties has also aroused interest, and a great number of tribocorrosion studies have taken place over the last decade to evaluate the performance of coatings produced by different depositing techniques (HVOF, PVD, etc.) [27, 35–37]. Finally, the increasing impact and growing interest of biomedicine over the last decade have led to a great number of studies involving biomedical alloys used in orthopaedic and dental implants [2, 38–40], which are subjected to both corrosion and wear as a result of human activity. Biomedical materials such as the CoCrMo [41–43] alloy or titanium alloys [44–46] have been widely studied in simulated body fluids (SBF), e.g., artificial saliva, NaCl solutions, phosphate buffer saline (PBS) solutions, or foetal bovine serum (FBS) solutions.

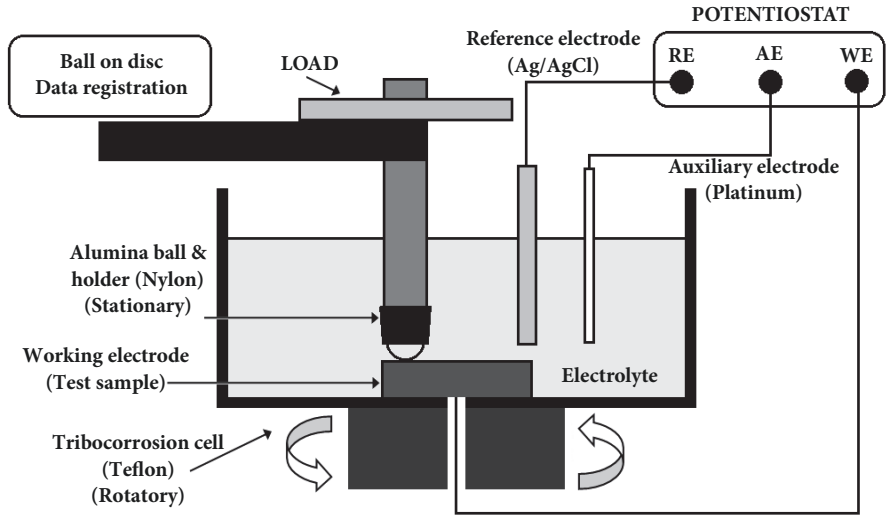

Figure 1: Schematic of a unidirectional tribocorrosion ball-on-disc experimental setup.

2.4. Tribocorrosion Test Procedures. The test procedures employed to assess tribocorrosion behaviour of passive materials involve performing and combining different electrochemical techniques. In general, tribocorrosion tests consist of analysing the electrochemical behaviour of surfaces before and during the tribological process, in order to evaluate how wear influences the electrochemical response of materials exposed to specific corrosive media, under determined mechanical conditions. The most widely used electrochemical techniques in tribocorrosion evaluation are potentiodynamic and potentiostatic tests, electrochemical impedance spectroscopy (EIS), open circuit potential registration (OCP), and electrochemical noise (EN) analysis.

The following sections explain how the electrochemical techniques used in tribocorrosion studies are combined. The sections have been divided into tests under controlled potential and tests under open circuit conditions. The different electrochemical techniques and their usefulness are described, and studies performed in tribocorrosion fields and relevant findings are included at the end of each section. The following section collects the current standardized tribocorrosion test procedures. The last sections provide a brief insight into the different approaches and models for tribocorrosion phenomenon proposed over the last few decades plus future perspectives.

3. Tribocorrosion Tests under Controlled Potential

3.1. Potentiodynamic Polarization Tests. The potentiodynamic polarization technique is one of the most widely used test methods to evaluate corrosion. It consists of putting a potential between the reference and working electrodes, in a potential difference range from the cathodic to the anodic domain at a constant sweep rate, while registering the current being produced. In these tests, the current represents the rate of the anodic or cathodic reactions that are taking place on the working electrode surface, i.e., the studied metal exposed to the corrosive electrolyte. The registered current is typically expressed in terms of current per unit area of the working electrode, that is, the current density [47]. This technique provides information about the different corrosion processes taking place on the surface of a metal, such as pitting occurrence susceptibility, passive layer formation, and the cathodic behaviour of an electrochemical system. It is the most useful method to evaluate the active/passive behaviour of the materials at different potentials and to determine the kinetics of ongoing reactions, i.e., the corrosion rate [10, 20, 48].

Performing potentiodynamic polarization tests during wear experiments can be used to evaluate the effect of wear on the electrochemical reactions on the surface of the working electrode, as a function of the potential applied, while being rubbed against an insulating body. Therefore, it is a quick and useful tool to detect the possible effects of friction on the electrochemical kinetics of the system, and vice versa [11, 49]. As a first approach, the current registered during potentiodynamic polarization in a material subjected to a sliding process is the sum of two components, namely, the currents of the worn and unworn areas. Furthermore, the coefficient of friction usually varies with applied potential during a potentiodynamic scan, due to the electrochemical changes taking place in the surface state of the material in the tribological contact [3, 50].

Figure 2(a) shows an example of a polarization curve obtained for a Monel K500 alloy in artificial seawater under corrosion-only and tribocorrosion (wear and corrosion) conditions. It can be clearly seen that, under tribocorrosion conditions, the corrosion potential is shifted to more cathodic potentials, and the corrosion current density is increased by two orders of magnitude [29]. Furthermore, there is a

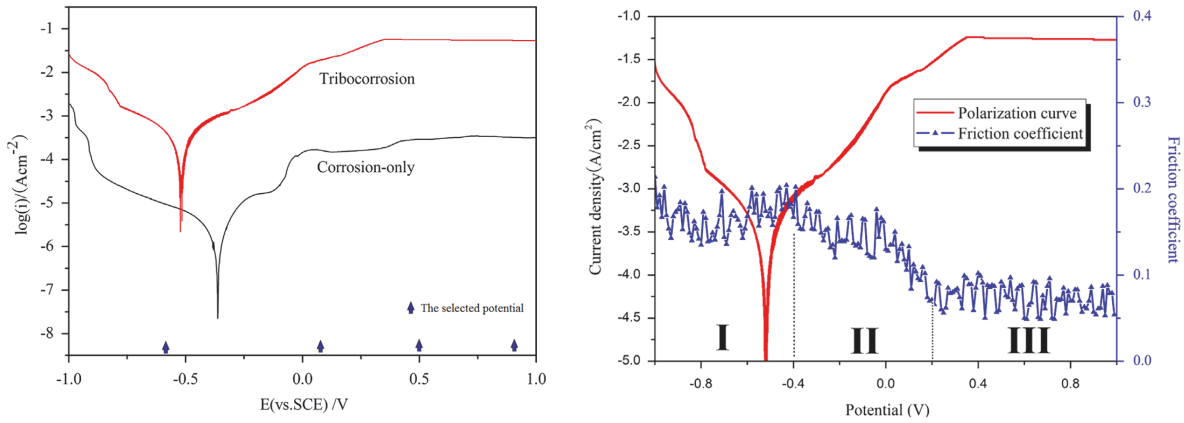

(a) (b)

Figure 2: (a) Polarization curves of a Monel K500 alloy in artificial seawater obtained in corrosion-only and tribocorrosion conditions. (b) Polarization curve of Monel K500 alloy in artificial seawater and evolution of coefficient of friction obtained during measuring. The corrosion potential under tribocorrosion conditions is shifted to more cathodic potentials, and the corrosion current density increases by two orders of magnitude. The coefficient of friction decreases with higher anodic potentials as a consequence of the presence of oxide film on the surface [29].

correlation between the coefficient of friction and the current density arising from the polarization imposed (Figure 2(b)). In this case, the coefficient of friction decreases at higher anodic potentials, as a consequence of oxide films forming on the surface [29]. Thus, the potentiodynamic polarization technique performed with and in the absence of sliding provides interesting information on both the effect of wear on corrosion and the influence of corrosion on wear behaviour.

3.2. Potentiostatic Polarization Tests. Electrochemical polarization is used to simulate the oxidizing action of a corrosive environment. This technique consists of imposing a fixed potential between the reference and the working electrodes. The current is measured as a function of time, to evaluate the evolution of electrochemical kinetics of reactions occurring on the electrode surface [11]. The potential value being applied determines the dominant electrochemical reactions taking place. The polarization curve of passive materials can be divided into three regions:

(i) Active region, where the metal dissolves directly in contact with the solution

(ii) Passive region, where a protective passive film of few nanometres is grown on the surface, protecting the bare material from dissolution

(iii) Transpassive region, at high anodic potentials, where the current increases sharply with potential, as a consequence of the nonstable state of the oxide layer and the breakdown of this film.

These three regions are clearly observed in the polarization curve represented in Figure 3, with i_{corr} the corrosion current density, E_{corr} the corrosion potential, i_p the current density in the passive state, and E_{pit} the potential at which pitting processes begin in the passive layer.

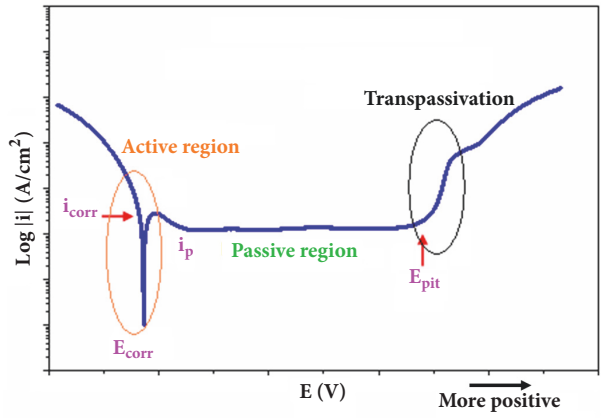

Figure 3: Typical Polarization curve of a passive material showing the active, passive, and transpassive regions.

Imposing a fixed potential on rubbing surfaces gives information on the potential effect on the wear behaviour [7]. The current registered during rubbing mainly flows through the wear track area, which constitutes a very small area compared to the complete metal surface exposed to the electrolyte [11]. The measured current value corresponds to the sum of the anodic and cathodic currents, due to all electrochemical reactions occurring on the exposed surface. It is thus possible to simulate different corrosion conditions by imposing appropriate potentials [7, 11, 49]. At cathodic potentials, the corrosion is inhibited, and the material loss after the tribocorrosion tests is attributed to pure mechanical wear. On the contrary, at anodic or passive potentials, the metal is covered by an oxide film whose thickness is controlled by the applied potential. This layer reduces the dissolution rate of the metal to negligible values and affects the friction response of the material.

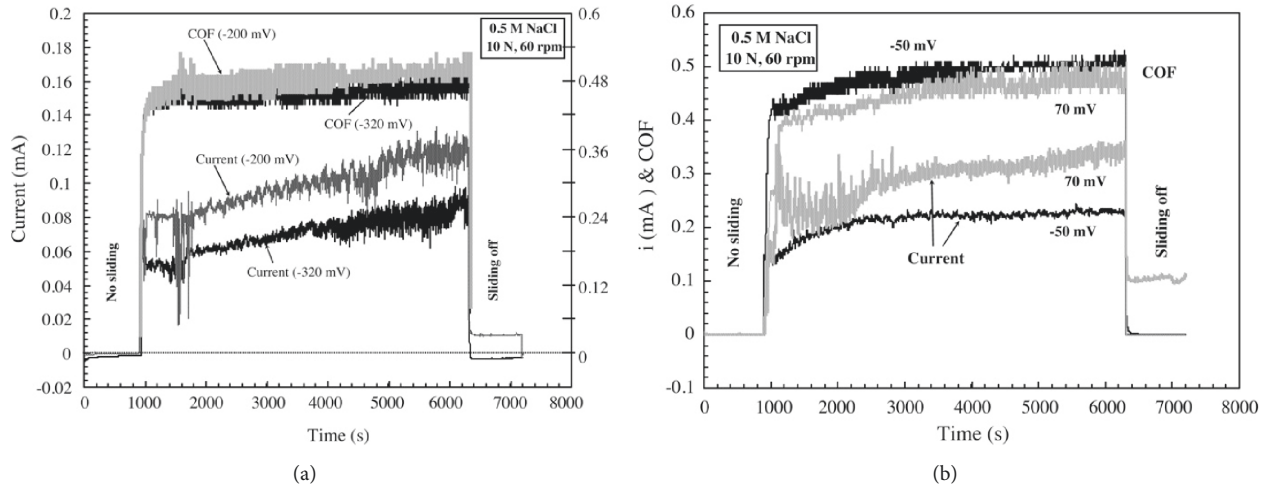

Figure 4: Current transients and coefficients of friction (COF) recorded before, during, and after sliding wear test at fixed potentials for an AISI 304 stainless steel in 0.5M NaCl solution: (a) -320 mV and -200 mV; (b) -50 mV and 70 mV. Removing the passive layer generates an increase in the current transient, with higher shifts at higher applied potentials. The coefficient of friction also varies with applied potential [24].

During sliding, the registered anodic current increases as a consequence of the local damage or removal of the passive layer exposing the base material surface to the electrolyte and, thus, to an active dissolution [3].

The evolution of current transient and coefficient of friction during sliding wear tests at different fixed potentials is shown in Figure 4, for a AISI 304 stainless steel in 0.5M NaCl solution [24]. Sliding results in a shift of current transient towards more positive values as a consequence of removing the passive layer, and this shift becomes higher as greater potential is applied. Moreover, the coefficient of friction value is also variable depending on the potential.

Additionally, this technique can also quantify the metal dissolution rate, i.e., the corrosion rate, from the corrosion current density (i_{corr}) registered using Faraday's law [4, 7, 11, 13, 21, 22, 48]:

$$v_{corr} = \frac{i_{corr}.M}{n.F} \quad (1)$$

where v_{corr} is the corrosion rate, M the atomic mass, n the number of electrons taking part in the process, and F the Faraday constant (96500 coulomb per electron mol). More details on calculating corrosion rates from electrochemical measurements can be found in the ASTM G102 [51] Standard.

3.3. Combination of Potentiodynamic and Potentiostatic Polarization Techniques to Assess Tribocorrosion. A wide number of researchers have combined polarization techniques for tribocorrosion evaluation of different passive materials in a wide variety of solutions. The polarization curves obtained from the potentiodynamic scan provide information on the electrochemical state of the material in a specific electrolyte at the different potential ranges. From the curves obtained in these tests, different potentials can be selected, namely, cathodic or passive potentials, to perform the potentiostatic tests under wear conditions. Some authors have also performed sliding wear tests at open circuit potential in combination with these two techniques, in order to acquire information on the potential evolution with sliding and evolution of the friction coefficient under free conditions. This technique is explained in more detail in the following section.

Former studies in the tribocorrosion field consisted of analysing the passivation phenomenon. As a first approach, understanding the formation of the passive film and its behaviour under corrosion-wear solicitations was the main interest. In the following studies, the influence of different chemical and tribological parameters on the tribocorrosion response was assessed, i.e., the effect of potential, velocity and normal load, or the test solution. Some studies performed by combining these two techniques over the last few decades and their major findings are detailed below.

3.3.1. Study of Passivation Phenomenon in Tribocorrosion. Understanding passivation drew attention from a great number of researchers in the tribocorrosion field from the outset. P. Jeremy et al. (2000) [23] studied the influence of passivation on tribocorrosion for an iron-chromium (AISI 430) alloy in sulphuric acid by measuring the current during rubbing under applied cathodic potential. They modelled the shape of the current transient considering the ohmic effects and the film growth kinetics and demonstrated that the repassivation kinetics determined the chemical metal removal rate under tribocorrosion conditions. A similar deduction was made by Mischler et al. (2001) [22] for a 34CrNiMo6 carbon steel in different aqueous solutions (NaOH and borate buffer solutions). They observed that passivity determined chemical degradation of both the metal and the detached metal wear particles and also played a crucial role in the mechanical properties of the metal surface. In 2001, Mischler and Ponthiaux [16] confirmed the reproducibility and

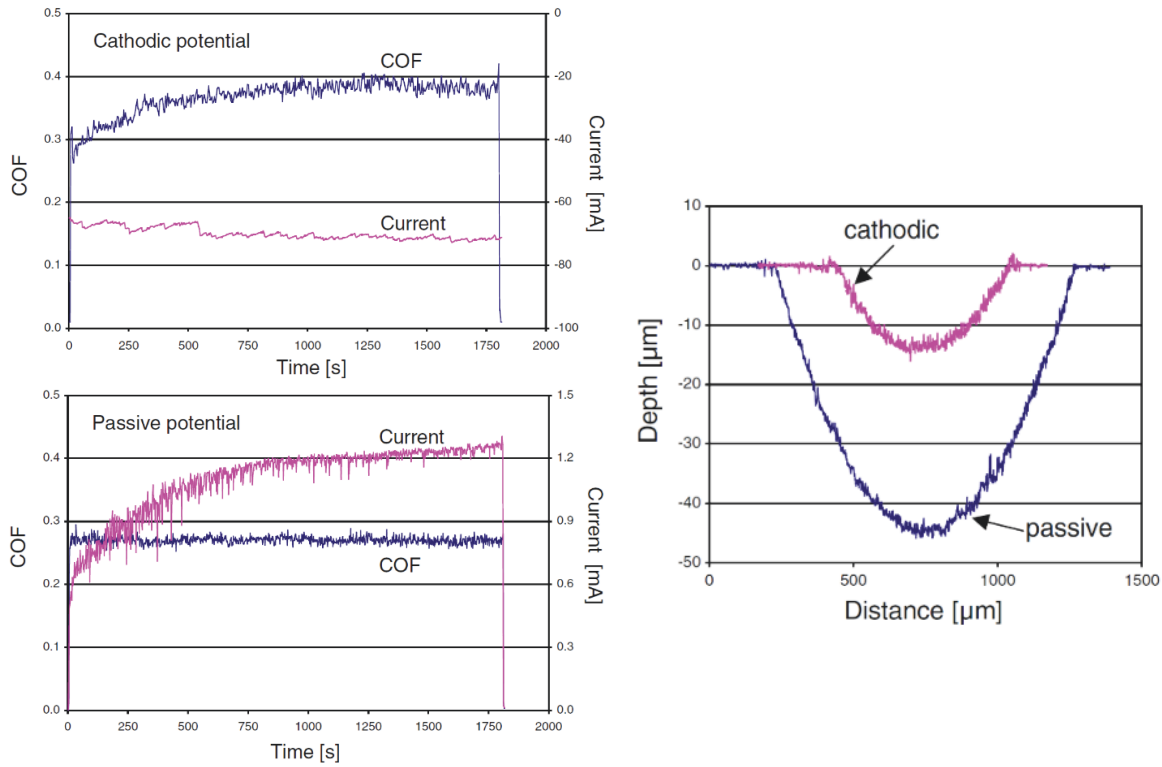

Figure 5: Effect of potential on the coefficient of friction and current during sliding (left) and on the wear track volume for a 316L steel in H_2SO_4 at cathodic (-1.5V) and passive (0V) potentials. The current values recorded are higher and the coefficient of friction is lower for passive potentials. The material loss at passive potentials is considerably higher due to wear-accelerated corrosion [55].

compatibility of tribocorrosion experiments analysing the electrochemical and tribological response of the AISI 316 alloy in sulphuric acid in seven different laboratories. They observed identical trends in the tribocorrosion behaviour of the alloy, an increase in passive current during rubbing, which they found to be proportional to the extent of the wear. For the same material/electrolyte system, García et al. (2001) [52] also observed sliding to cause both a potential shift to more anodic values in the polarization curves and an increase in the current values in the potentiostatic tests. They proposed the concept of active wear track to describe the depassivation-repassivation processes taking place in the contact and demonstrated that there was no need to calculate the real wear contact area. They asserted that it was possible to determine this active area by electrochemical means, using the anodic current registered during sliding corrosion-wear tests under applied potential.

3.3.2. Influence of the Electrochemical Potential, Solution Chemistry, and Sliding Velocity and Normal Load on Wear and Wear-Accelerated Corrosion. Independently of the material and solution studied, the applied potential has been found to have an important effect on wear and wear-accelerated corrosion, as a consequence of the electrochemical state of the surface, i.e., free of oxides at cathodic potentials or covered by an oxide film in the passive domain. Stemp et al. (2003) [21] investigated the effect of contact configuration and observed that the metal loss rate was governed by the rate of mechanical depassivation. The repassivation rate, in turn, was found to be critically affected by sliding velocity and by the behaviour of the material in the wear track, which depended on the applied potential [53]. Barril et al. (2005) [54] and Favero et al. (2006) [55] observed that the extent of wear was profoundly affected by the applied potential, with higher material losses due to wear-accelerated corrosion at potentials above the corrosion potential (Figure 5). Similar observations were made for different material/electrolyte systems, by other researchers [29, 56]. Bidiville et al. (2007) [57] continued the study of Favero [55], and they further observed that the presence of a passive film affected the plastic deformation and the wear track behaviour. The metal under cathodic potential, free of oxides, was rapidly work-hardened under the applied load, and the plastic deformation resulted in limited wear. Furthermore, the wear rate was greater under passive potential due to subsurface cracking and limited plastic flow as a consequence of the passive film. Therefore, the wear rate and friction of materials can be controlled with the use of the right electrochemical potential, which could be a useful tool in industrial applications to reduce friction in certain components, as confirmed by Ismail et al. (2009) [58].

On the other hand, several studies have shown that the tribocorrosion rate also depends on the chemistry of the test solution. Espallargas and Mischler (2010) [59] investigated the passivation of an overlay-welded Ni-Cr 625 alloy in

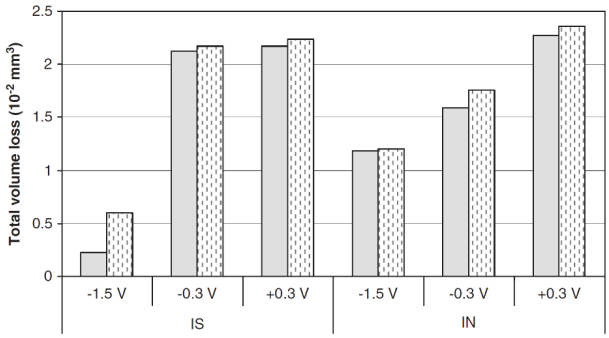

Figure 6: Total volume loss for an overlay-welded Ni-Cr 625 alloy under 15N at different applied potentials in sulphuric acid (IS) and nitric acid (IN) solutions. The material loss in IS at cathodic potentials is considerably smaller than at passive potentials, whereas this effect is less pronounced in IN, where the wear rate increases steadily with applied potential [59].

sulphuric and nitric acids, at different potentials (Figure 6). The tribocorrosion damage in sulphuric acid was observed to be less under cathodic conditions, and no effect of potential in the passive region was found. In nitric acid, however, similar wear was observed in passive and cathodic potentials. This was attributed to the oxidizing action of nitrate ions that helped form an oxide film layer even under cathodic polarization, which was found to cause wear. Muñoz and Julián (2010) [48] studied the corrosion resistance of the CoCrMo alloy in NaCl and a bovine serum (BS) solution under potentiostatic control at different applied potentials. They observed that the tribocorrosion rate depended on both the applied potential and solution chemistry. Wear was almost negligible at cathodic potentials and increased critically with increasing potentials, and the properties of the passive film were different depending on the solution chemistry, thus modifying the tribocorrosion behaviour of the alloy. Chen and Yan (2012) [31] performed tribocorrosion tests on Ti-6Al-4V and Monel K500 alloys against a 316 stainless steel in artificial seawater and distilled water. They found that the coefficient of friction was lower in seawater, as a consequence of the increase in surface roughness due to higher corrosion, which led to a reduction in the contact area. Golvano et al. (2015) [60] evaluated the effect of fluoride content and solution pH on the corrosion and tribocorrosion behaviour of titanium alloys in artificial saliva. The increase in fluoride content and the acidification of the saliva were found to have a negative effect on corrosion resistance of the alloys.

In addition to electrochemical potential and solution chemistry, tribological conditions such as sliding velocity or applied normal load also affect the tribocorrosion behaviour of materials. Radice and Mischler (2006) [61] found that the wear rate increased with increasing load and electrochemically applied potential. Sun and Rana (2011) [24] reported that the cathodic shift in the potential due to the sliding was greater with higher sliding speeds and contact loads. Dahm (2007) [62] observed that the corrosion current did not depend linearly on the wear scar area, and the electrochemical contribution increased with increasing sliding distance. Therefore, the wear-corrosion synergies were not a fixed proportion of the total wear. Yue et al. (2014) [30] analysed the influence of microstructure evolution on the tribocorrosion behaviour of a stainless steel, and the strain-induced microstructure changes occurring during sliding were found to affect the synergistic degree of wear and corrosion.

3.3.3. Bio-Tribocorrosion. Interest in studying tribocorrosion in the biomedical field has increased over the last few decades. The major bio-tribocorrosion areas are orthopaedic science and dentistry. In both cases, the main goal is to develop or select a biocompatible material that can resist both wear and corrosion conditions for the human body, assuring certain durability with the lowest metal ion release. However, the study of bio-tribocorrosion is quite complicated, since it involves the composition of human fluids containing bacteria, proteins, and so on, leading to a more complex system with several influencing parameters.

As mentioned in the previous section, the electrode potential can affect the wear rate of materials in tribocorrosion systems. This effect has also been observed in bio-tribocorrosion studies, where the metal ion release under wear-corrosion conditions of the human body critically depends on the electrode potential, as confirmed by Espallargas et al. (2015) [63]. On the other hand, the proteins present in human body fluids have been found to have a beneficial effect on the tribocorrosion response for biomedical materials. These proteins have been found to form a biofilm on the alloy surface, composed of inorganic graphitic carbon, which acts as a boundary lubricant [64]. However, high applied potentials and normal loads can inhibit the lubricating ability of the proteins, as observed in several studies such as Liau et al. [64], Hiromoto and Mischler (2006) [65], Mathew et al. (2011) [66], or Sadiq et al. (2015) [67]. As reported by Runa et al. (2013) [68], the effect of proteins can be either favourable or undesired, depending on the characteristics of the passive film formed at different applied potentials under mechanical exposure.

4. Tribocorrosion Tests at Open Circuit Potential

The open circuit potential (OCP) is the spontaneous potential established between the working and the reference electrodes, at which anodic and cathodic reactions take place in an electrochemical system. This parameter does not give information on electrochemical reaction kinetics but indicates whether a material is noble or active in a determined electrolyte. Tribocorrosion tests at open circuit potential consist of performing sliding wear on a material immersed in a specific electrolyte, without imposing any anodic or cathodic potential [3, 11, 20]. There are three main techniques used in a wear tests at open circuit potential: OCP monitoring with and without wear, electrochemical impedance spectroscopy (EIS) measurements, and electrochemical noise (EN) technique.

4.1. Open Circuit Potential Monitoring. The open circuit potential monitoring is the simplest electrochemical method for corrosion evaluation, although it does not provide quantitative information on the interaction between wear and corrosion. To study the effect of wear, the potential is monitored before, during and after the sliding. Before the sliding test, the samples are immersed in the electrolyte until a steady state is achieved. Several authors have performed experiments with an hour of stabilisation [3, 10, 11, 20]. However, the stabilisation period depends on the material and electrolyte used and should be selected considering the system being studied. The potential evolution registered during the stabilisation period provides information on the electrochemical reactivity of the material in the test solution. An increase in the potential with immersion time reaching stable values after several minutes of immersion indicates the formation of a passive oxide layer on the surface. This layer of a few nanometres protects the material underlying from corrosion. This phenomenon is known as passivation [3, 10, 11, 20]. On the other hand, a decrease of potential with immersion time suggests that general corrosion has occurred. Finally, short-term potential fluctuations are attributed to localized corrosion processes such as pitting. These fluctuations are a consequence of the successive breakage of the passive layer and subsequent growth of the film in the affected zone [10, 12, 38]. The reaction time can be calculated using the potential evolution curve meaning the time needed upon immersion to reach a stable potential for the tested material in the selected media [3, 10, 11, 20].

Measuring potential during sliding can also provide information on the evolution of surface state when the material is subjected to wear-corrosion conditions. Once sliding begins, the potential has been observed to shift towards more negative values, indicating the initiation of electrochemical activity. Change in potential is a consequence of removing the passive layer in the tribological contact, thus exposing the bare material to corrosion. During wear, galvanic coupling between the active worn area and passive unworn area is generated [3, 10, 11, 20]. According to Ponthiaux et al. [20], there are four parameters that affect the corrosion potential during rubbing:

(i) The intrinsic corrosion potentials of the unworn and worn surfaces where the electrochemical state of the worn surface is disturbed by the removal of the passive layer and the mechanical strain caused by sliding

(ii) The ratio between worn and unworn surface areas

(iii) The relative position between worn and unworn areas

(iv) The mechanisms and kinetics of the anodic and cathodic reactions involved in the worn and unworn areas.

After sliding, the potential usually tends to increase again reaching values close to presliding figures, as a consequence of the reformation of the passive layer in the depassivated area. The potential restoration process gives information on the material's ability to recover after sliding, which is known as repassivation.

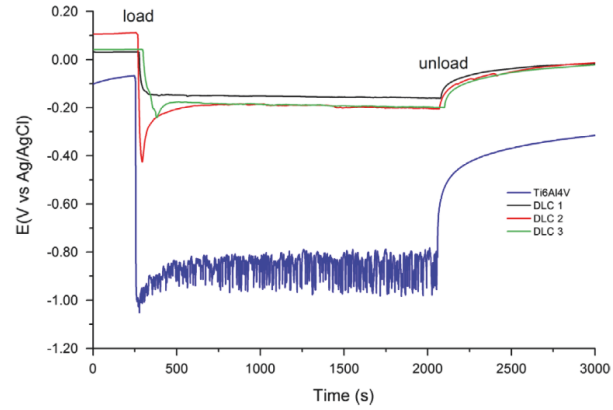

Figure 7: Evolution of the open circuit potential before, during, and after sliding wear test for a Ti6Al4V alloy with different DLC coatings in PBS solution. Sliding removes the passive layer on the surface, leading to a decrease in the potential value. At the end of sliding, the material is repassivated, and the potential increases to reach values close to those before sliding [69].

The shift in potential due to the action of wear can be clearly observed in Figure 7, for a Ti6Al4V alloy with several DLC (Diamond Like Carbon) coatings in Phosphate Buffered Solution (PBS) [69]. As soon as the countermaterial begins to slide against the test materials, a depassivated area is created in the surface leading to a decrease of potential due to the galvanic couple generated between the worn and unworn surfaces. Once sliding ends, the potential increases again to reach potential values close to those before wear process, as a consequence of the repassivation of the surface.

4.2. Electrochemical Impedance Spectroscopy. The electrochemical impedance spectroscopy (EIS) technique consists of exciting the system using an AC potential or small amplitude current sinusoidal signal over a wide range of frequencies and measuring the current or potential response obtained. This technique is usually performed at free potential, with the requirement that the material should be electrochemically stable, in terms of the open circuit potential. Therefore, a small amplitude, usually 5-10 mV, is employed to maintain the system in a (quasi)equilibrium state. As a consequence, the system can be evaluated without imposing significant perturbations. The impedance spectrums are obtained by plotting the electrochemical impedance, i.e., the potential and current ratio, over the frequency range being studied. The spectrums are then modelled using equivalent electric circuits that combine passive electric elements such as resistors, inductors, and capacitors. Combining the elements reproduces the electrochemical behaviour of the electrode surface. Information on the elementary steps occurring in the electrochemical reactions and their kinetics can also be obtained from the impedance diagrams [3, 10, 20, 70–72].

One of the diagrams used to represent impedance data is the so-called Nyquist plot, where the imaginary impedance, indicative of capacitive response, is represented versus the real impedance, which indicates a resistive response. Figure 8

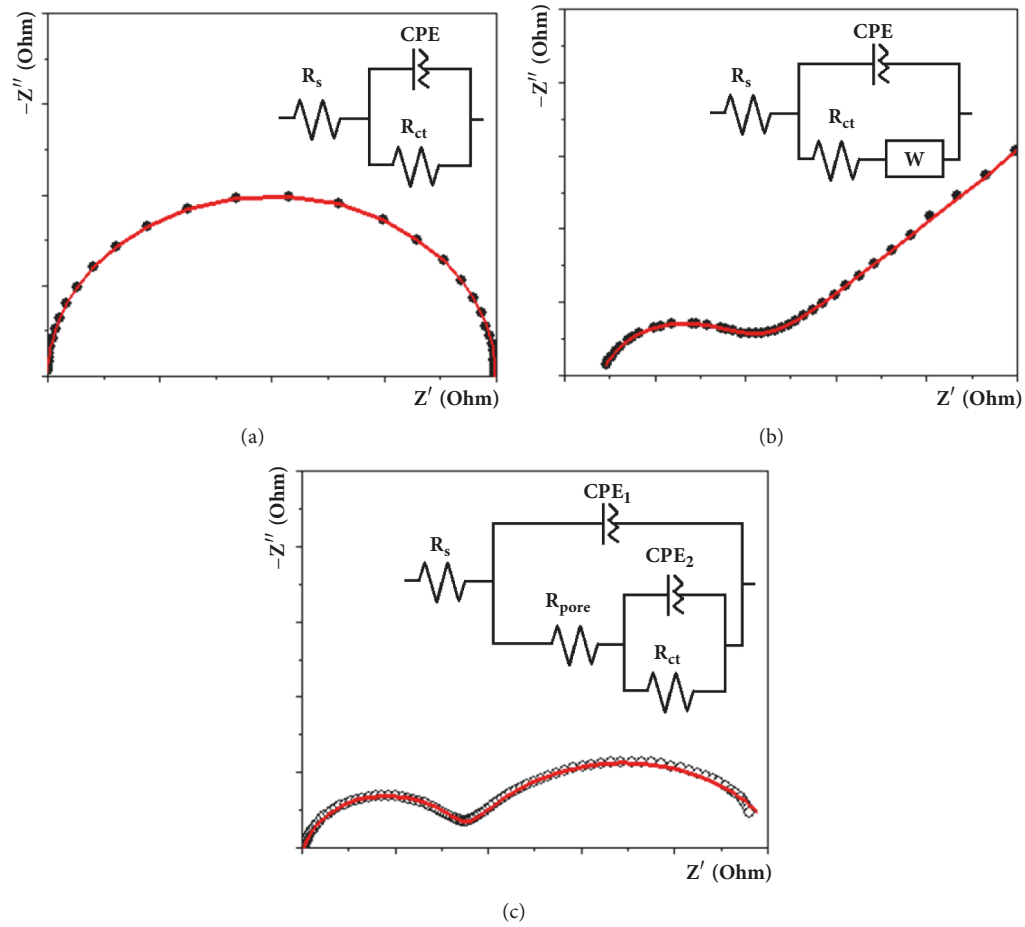

Figure 8: Nyquist plots for impedance data and equivalent circuits used to fill each curve for a metal or alloy (a) without any coating, (b) without a coating showing diffusion of reactants, and (c) with a passive oxide layer or a porous coating on the surface.

shows typical Nyquist diagrams, together with the electrochemical equivalent circuit used in each curve to fit the impedance data. Figure 8(a) represents a bare metal without any coating, (b) shows the response of a metal or alloy with mixed activation and diffusion control, and (c) is the case of a metal with a protective oxide layer or a porous coating on the surface. In the equivalent circuits, R_s represents the solution resistance, CPE is the constant phase element representing the capacitive properties of the electrolyte/metal interface, and R_{ct} is the charge transfer resistance in the electrolyte/metal interface, which determines the kinetics of the reaction. The Warburg impedance (W) in Figure 8(b) indicates the occurrence of reactant diffusion to the corroding surface, as a consequence of reactant concentration gradients in the solution. In the last circuit (Figure 8(c)), CPE_1 corresponds to the capacitance of the coating, whereas CPE_2 is the capacitive properties of the electrolyte/metal interface. Finally, R_{pore} is the resistance of the paths generated in the coating, i.e., the resistance in the pores.

This technique can be used to study the role of intermediate species adsorbed in the surface, the properties of the passive films generated, and also the changes in the metal/electrolyte interface. The high frequency loop is associated with the charge transfer taking place in the interface, whereas the low frequency loop is attributed to diffusion of dissolved oxygen from the electrolyte to the metal/electrolyte interface [20, 48].

By performing impedance measurements during sliding, it is possible to study the influence of wear on the elementary processes involved in the corrosion mechanism. Analysing the changes in the impedance diagrams with sliding parameters, i.e., normal force or sliding speed, it is possible to develop a model taking into account the effects of sliding in the corrosion mechanism [10, 50]. On the other hand, the EIS measurements after sliding provide information on the recovery of the material in post-wear damage. The approximate value of corrosion current (I_{corr}) or passivation current (I_{pass}) of a metal or alloy can be determined from the polarization resistance (R_p). This value is obtained from the impedance diagrams. EIS is the most accurate technique among the different methods available to measure the polarization resistance [10].

The effect of wear on corrosion can be observed in the Nyquist and Bode plots in Figure 9. The results correspond to EIS measurements performed before and during sliding of a TaN-coated and uncoated titanium alloy in PBS solution [73]. The electrochemical data was fitted with the so-called Randles equivalent circuit.

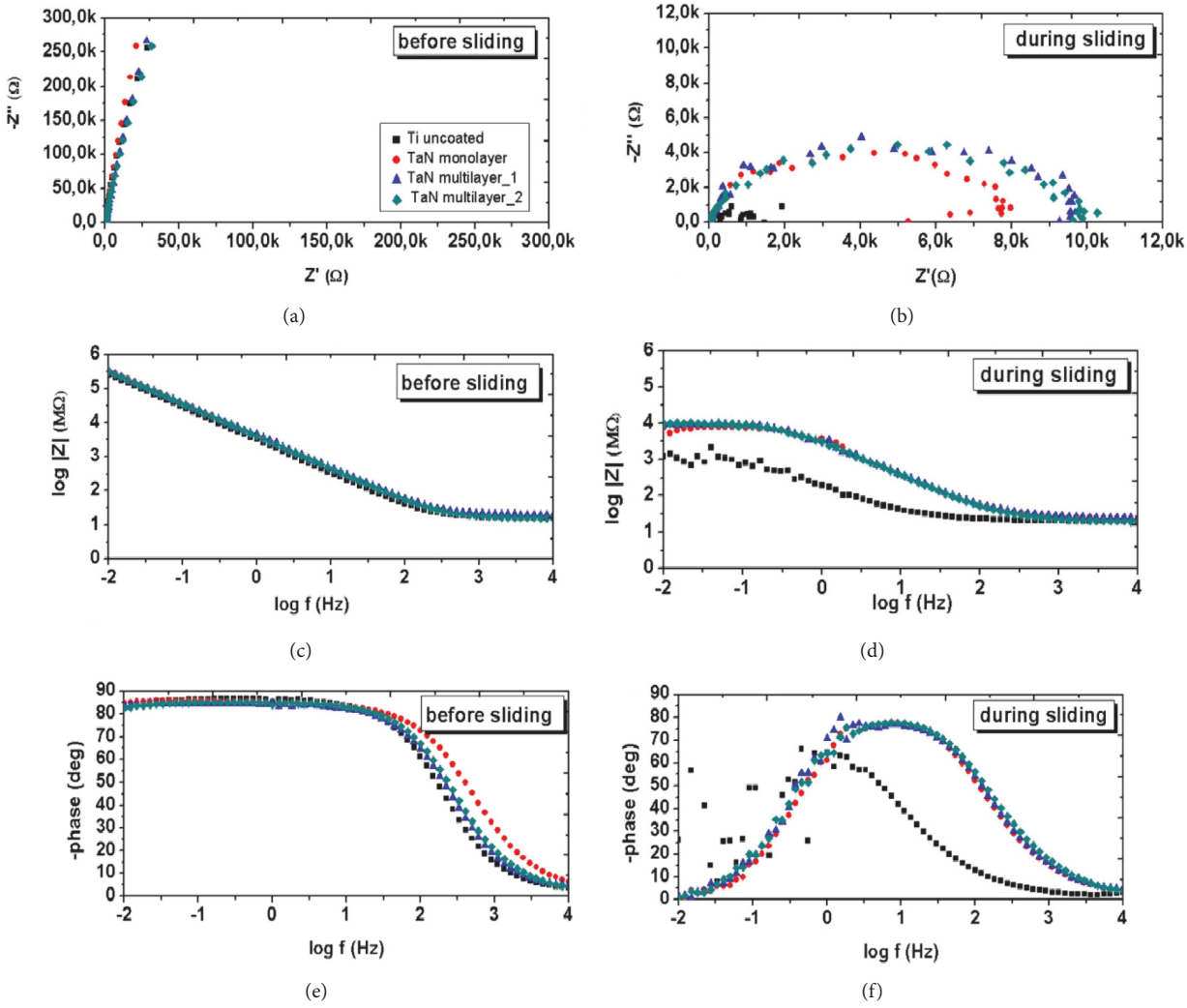

FIGURE 9: Nyquist and Bode plots of the EIS measurements performed before (a,c,d) and during (b,d,f) sliding process, for a titanium alloy and a TaN-coated titanium alloy in PBS solution. A decrease in the resistance is observed due to wear processes in both titanium and TaN coatings, but the resistance of the coatings was an order of magnitude higher than for the uncoated alloy [73].

4.3. Combination of Open Circuit Potential Monitoring and Impedance Measurements. Due to its simplicity, the combination of OCP monitoring and EIS measurements has been widely used in tribocorrosion studies. These tests usually consist of monitoring the potential until a steady state is reached, and registering the potential response during the wear test, and several minutes after the end of wear to study the depassivation and repassivation phenomena. These measurements are combined with EIS measurements before, during, or after sliding, to evaluate the effect of wear on the corrosion response of the system.

By combining OCP and EIS measurements, M. Azzi and J.A. Szpunar (2007) [39] observed that the nitriding process applied on a titanium alloy enhanced the corrosion resistance of the alloy. R. Bayón et al. (2009) [74] compared the tribocorrosion response of different Cr/CrN multilayer coatings in NaCl solution and observed the influence of the layers' thickness on the wear-corrosion behaviour. R. Bayón et al. (2015) [69] studied the enhancement on corrosion and tribocorrosion performance of different Ti-DLC coatings deposited on Ti6Al4V biomedical alloy in simulated body fluids. M.J. Runa et al. (2015) [75] evaluated the role of organic materials (osteoblastic cells) on the bio-tribocorrosion performance of a Ti6Al4V alloy in simulated body fluids and observed that the layer formed by the osteoblastic cells improved the wear and corrosion performance of the alloy. V. Saenz de Viteri et al. (2016) [76] analysed the tribocorrosion behaviour of TiO_2 coatings containing osseointegration enhancing (calcium and phosphorous) and antibacterial (iodine) elements generated by plasma electrooxidation (PEO) technique and observed an improved wear resistance for one of the developed coatings (Figure 10).

Several researchers have also combined potentiodynamic polarization techniques with open circuit potential and electrochemical impedance spectroscopy measurements. N. Papageorgiou et al. (2014) [77] analysed the tribocorrosion

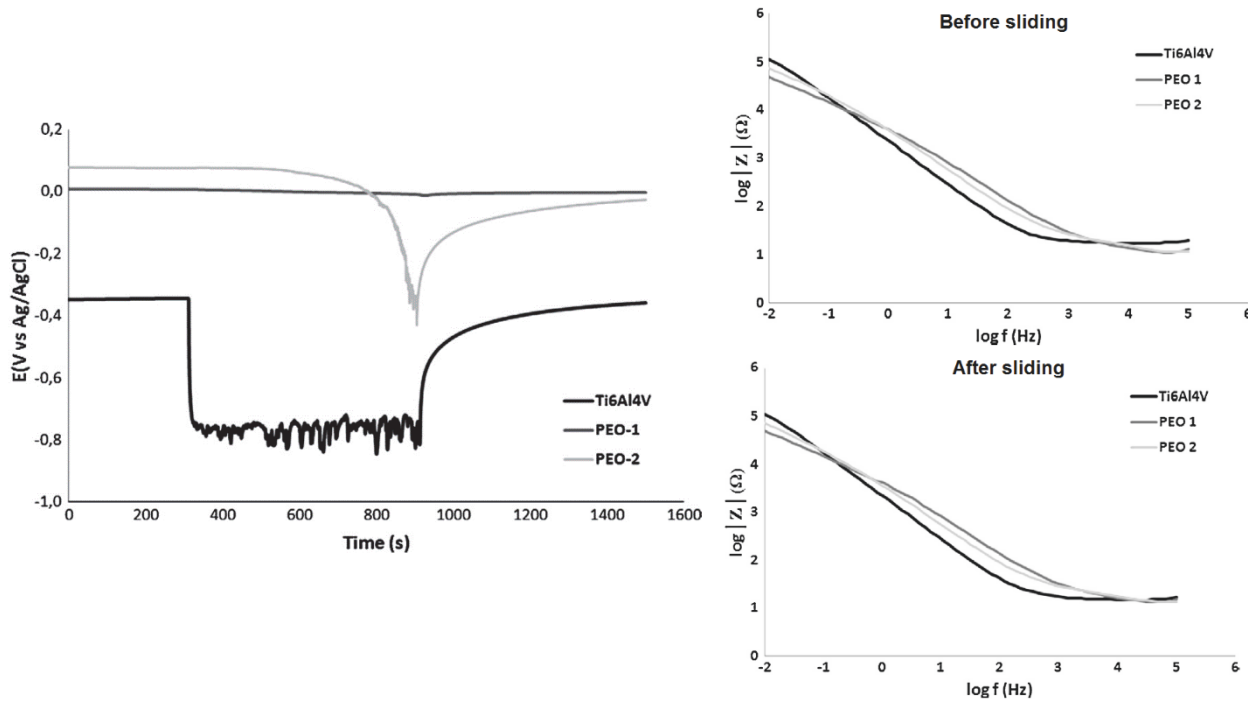

Figure 10: Potential shift towards more negative values due to a sliding process for a Ti6Al4V alloy with and without TiO_2 coatings generated by PEO technique in PBS solution (left) and impedance spectroscopy measurements obtained before and after sliding (right). The electrochemical state of the TiO_2 coating surface was not highly affected by sliding, and no influence of sliding on the corrosion resistance of either sample was observed [76].

performance of NiCrMo625 alloy in NaCl aqueous solution and proposed a triboelectrochemical model that proved the presence of debris particles. R. Alemón et al. (2015) [78] investigated the improvement of ion release of a CoCrMo alloy by a TiAlVCN/CN_x multilayer coating. M. Fazel et al. (2015) [79] observed an enhancement in the corrosion and tribocorrosion behaviour of titanium alloys treated by micro-arc oxidation process.

Finally, the literature also includes tribocorrosion assessment studies by just performing open circuit potential measurements before, during, and after sliding. S. Rossi et al. (1999) [80] compared the wear-corrosion behaviour of (Ti,Cr)N and Ti/TiN PVD coatings in sodium chloride solution. S.A. Alves et al. (2015) [81] investigated the response of titanium oxide films with different compositions to enhance the tribocorrosion behaviour of a titanium biomedical alloy. M.Buciumeanu et al. (2016) [82] studied the tribocorrosion behaviour of hot pressed CoCrMo biomedical alloy in artificial saliva and found the processing conditions to play a relevant role on the tribocorrosion response of the alloy.

4.4. Electrochemical Noise Analysis. Electrochemical noise (EN) can be defined as the spontaneous potential and current fluctuations taking place in a metal exposed to an aggressive medium. Most corrosion processes in metals are electrochemical and, thus, are likely to generate electrochemical noise. The use of the electrochemical noise technique to assess corrosion as an *in situ* nondestructive technique dates back to the late 70s and early 80s [40, 83, 84]. Electrochemical impedance spectroscopy and electrochemical noise technique are commonly used when the information obtained from direct current (DC) techniques is not enough to characterise the system. In other words, when the corrosion process takes place in a series of stages, other techniques such as potentiodynamic polarization just provide information on the corrosion rate of the controlling reaction, which is not enough to understand the mechanism of the reaction taking place [83].

The previously explained electrochemical techniques, i.e., potentiodynamic polarization, potentiostatic tests and electrochemical impedance spectroscopy, require an external potential source to perturb the system, by either accelerating or inhibiting the corrosion kinetics. The main advantage of the electrochemical noise technique is that the corrosive system is not disturbed externally by the measurement process, so the system is kept in the natural corrosion potential. Thus, it allows potential and current fluctuations to be registered simultaneously, so it is possible to obtain information on the thermodynamics from the potential noise and kinetics information from the current noise. EN measurements allow the early stages of localized corrosion to be detected and studied and can isolate the individual events related to film breakdown in the sliding zone [10, 40, 85, 86].

The electrochemical noise is a low frequency (<10 Hz) potential or current fluctuation of small amplitude, originating from the variation of electrochemical reaction rates in a

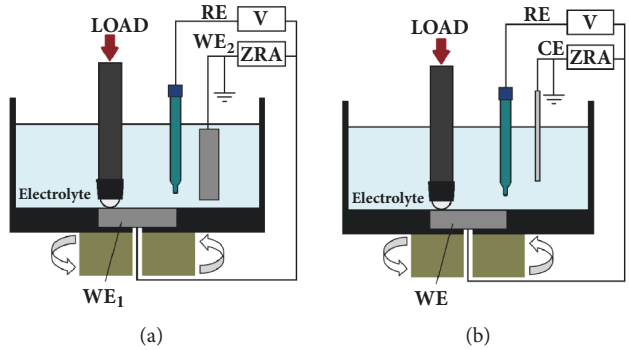

Figure 11: Schematic setup configuration for potential and current noise registration using: (a) two nominally identical electrodes and (b) asymmetrical electrodes.

corrosion process. There are several noise sources in corrosion [40, 85, 86]: atoms exchange kinetics in the electrode surface, the formation and release of bubbles on the surface, mechanical effects, formation of pits, transport fluctuations, temperature variations, variations on the solution resistance due to concentration gradients derived from the corrosion process, or the appearance of events controlled by nucleation, among others.

There are three main experimental configurations for simultaneous registration of potential and current signals. The configuration that has been most widely used in tribocorrosion assessment is schematically shown in Figure 11(a). It consists of using two working electrodes made of the same material (WE_1, WE_2). CE and RE are the counterelectrode and reference electrode, respectively. It is necessary to connect the two working electrodes through a Zero Resistance Ammeter (ZRA), which can measure the current while maintaining both working electrodes at a negligible potential difference. Two electrodes coupled through a ZRA will basically behave as a single electrode. The registered current signal corresponds to the current flowing between the two working electrodes, whereas the potential measured is the potential difference between both working electrodes and the reference electrode [84–87].

The local potential variations of each working electrode generate small variations in the mixed potential of the system. Therefore, the working electrodes must be nominally identical with the same surface preparation, since any difference would generate a galvanic couple, accelerating the oxidation of the more active electrode [84, 85]. In a tribocorrosion test, however, the electrodes are identical right until sliding wear process is initiated. Once wear is generated, the removal of the passive layer makes the worn electrode more active compared to the undamaged one. Therefore, the mechanical activation leads to galvanic coupling between the worn (anode) and unworn (cathode) electrodes. The latter acts as the cathode of the reaction, accelerating the corrosion-wear process on the worn sample [3, 40, 86, 88].

Sometimes, the different electrochemical characteristics presented in nominally identical electrodes generate asymmetry between them. In order to assess this drawback, several researchers have used asymmetric electrodes intentionally, measuring the electrochemical noise and studying the electrochemical processes taking place just in one of the working electrodes. For this purpose, platinum microcathodes have been widely used [40, 84, 86]. The configuration is schematically represented in Figure 11(b). The platinum microelectrode area must be small enough to avoid polarization of the working electrode, ensuring that the tribocorrosion process is not accelerated, and thus, current variations registered are the result of the mechanically influenced electrochemical process. Therefore, the electrochemical noise registered mainly belongs to the worn working electrode.

Figure 12 shows the response of current and potential before, during, and after sliding measured by electrochemical noise technique for a bare and duplex treated (plasma nitriding and deposition of CrN coatings) AISI 304 stainless steel in a Hank's Balanced Salt Solution (HBSS) [89]. In this study, the working electrode was coupled with a platinum microcathode through a ZRA.

4.4.1. Tribocorrosion Assessment by Electrochemical Noise Technique. Some investigators have used the above-mentioned configurations to evaluate the tribocorrosion behaviour of passive materials using the electrochemical noise technique. In these tests, the shifts in current and potential signals due to the sliding process are simultaneously registered. Several authors have also performed potentiodynamic tests in addition to EN measurements.

Galliano et al. (2001) [88] connected two identical working electrodes to a ZRA and performed the wear test on one of them. A reference electrode was used to measure the open circuit potential of the worn sample. The two originally identical samples became significantly different once a wear process started, generating galvanic corrosion between the two samples which, in turn, accelerated the tribocorrosion process. In one of the test configurations employed by Salasi et al. (2015) [90], they used the ZRA setup, coupling the test sample galvanically to a nominally identical electrode, and recording the current difference between the two samples. They observed an increase in the current and a cathodic shift of the free potential with the onset of abrasive particles to the sample. Thus, it was confirmed that the amount of current

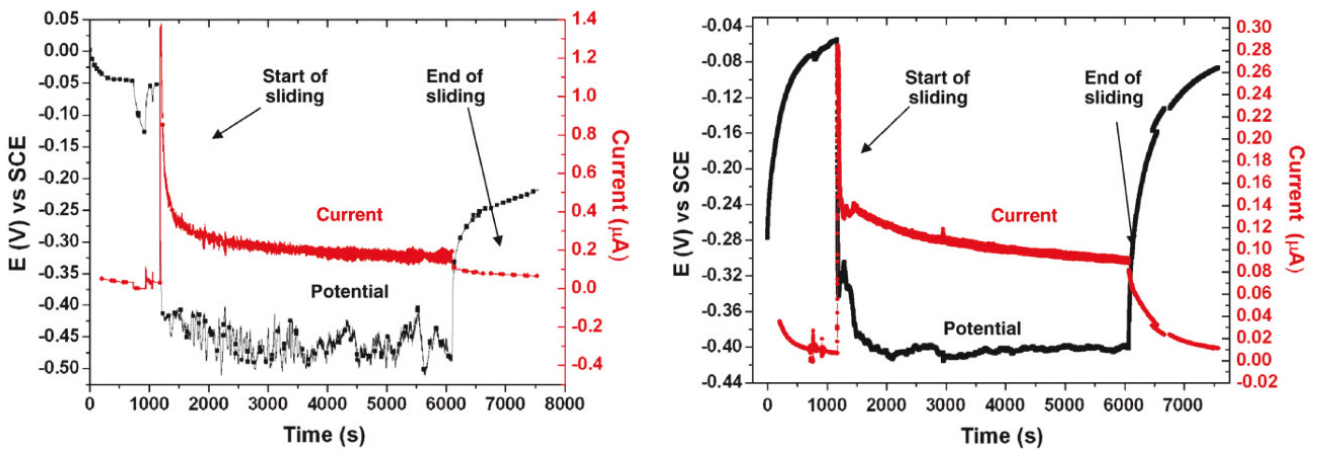

Figure 12: Potential and current response measured by electrochemical noise technique on (a) AISI 304 stainless steel and (b) duplex treated 304 against corundum in HBSS. In both cases, the potential decreases and the current increases during sliding, as a consequence of removing the passive layer and exposing the bare material to electrolyte [89].

discharge for this contact configuration was proportional to the number of particles that could successfully disrupt the passive film. Stachowiak et al. (2015) [9] studied the three-body abrasion-corrosion using several electrochemical techniques, discussing the benefits and limitations of each technique. They used two different methods based on measuring the EN: monitoring the galvanic current and potential noise of a freely corroding metal connecting two nominally identical electrodes and monitoring the current noise at an imposed anodic potential.

In order to avoid the asymmetry generated in the identical electrodes by the action of wear, Wu and Celis (2004) [86] coupled the working electrode to a platinum microelectrode. The microelectrode was used to record current variations during fretting experiments resulting from modifying the working electrode induced by sliding. This configuration allowed both potential and current responses to be measured during a fretting corrosion test, without accelerating the corrosion-wear of the tested materials. Therefore, the electrochemical noise technique was found to be useful to identify and/or unravel materials modification processes taking place during corrosion-wear sliding tests on passivating materials.

Several investigations have therefore been made by connecting the working electrode to a platinum microelectrode through the ZRA [28, 91–93]. Quan et al. (2006) [94] evaluated the corrosion-wear of TiN coated AISI 316 stainless steel in sulphuric acid solution and found that the corrosion-wear mechanism of the coatings depended on their substrate properties. They affirmed that the EN technique was a promising on-line monitoring tool that allowed delamination of a coating to be detected, since the interface between the coating and the substrate could be detected sensitively. Berradja et al. (2006) [95] used in situ electrochemical noise measurements to investigate the dependence of tribocorrosion on applied normal force and sliding velocity. The increase in the normal force and sliding velocity was found to induce an increase in the current and a decrease in the potential, accelerating the depassivation rate of the tested materials. From the electrochemical noise registered during tribocorrosion tests, A. de Frutos et al. (2010) [89] observed the activation of the worn surface when sliding started, and they attributed local current and potential variations during the steady-state phase to the oxide removal and repassivation process taking place in the wear track (Figure 12).

In an attempt to overcome a major drawback of ZRA measurements, i.e., the loop back effect of current lines that do not go through the ZRA apparatus but remain confined to the working electrode, Silva et al. (2011) [96] suggested a new test configuration. This setup consisted of exposing only the wear track to the electrolyte, by covering the working electrode with an insulating polymer film. Besides, they used a cylinder of the same material concentrically placed just above the working electrode. With this configuration, most of the cathodic current was forced to flow through the ZRA, since the WE acted as a continuously depassivated anode. With this setup, the load increase was found to increase the anodic current between the working and counterelectrode, which remained passive and reduced the potential.

Espallargas et al. (2013) [97] proposed a new experimental technique based on galvanic current and potential measurements through a ZRA, for quantifying the electrode potential and the anodic current inside the wear track during rubbing at OCP. The proposed experimental setup allowed them, for the first time, to determine the electrochemical conditions inside the wear track, i.e., electrode potential and anodic current. This was achieved by physically separating the cathode from the anode (wear track), by using two working electrodes: a coated steel sample where just the wear track was exposed to the electrolyte and an uncoated steel sample acting as the unworn area (Figure 13). The experimental setup was found to be suitable as a quantitative tool to determine both galvanic coupling parameters during

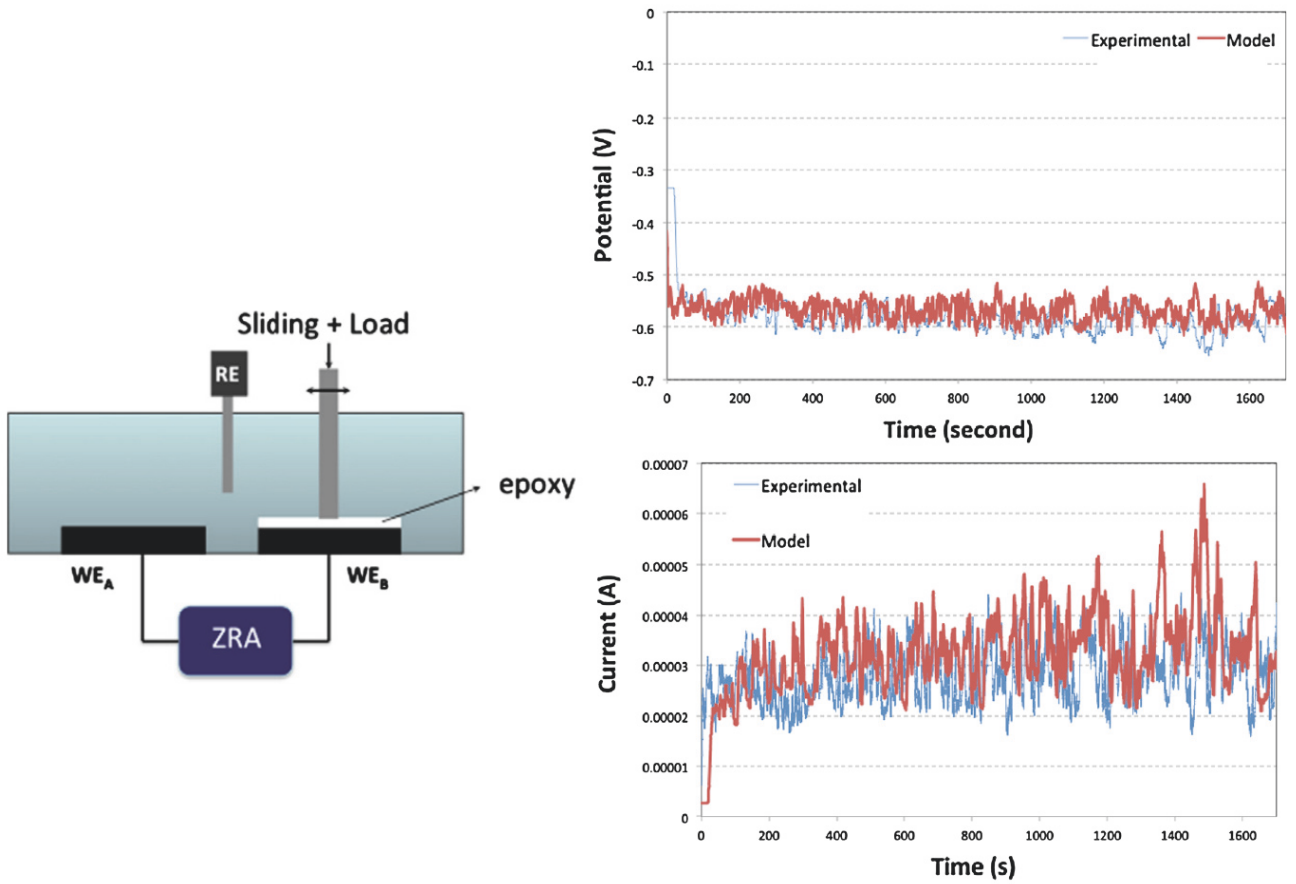

FIGURE 13: Left: schematic of the electrochemical setup used by Espallargas et al. [97] connecting the uncoated sample (unworn surface) and coated sample (wear track) through a ZRA. Right: potential and current evolution for a Ti6Al4V rubbed against an Al_2O_3 ball at 540 MPa in artificial saliva, obtained by Licausi et al. [98] using this setup. The experimental results and the simulated values.

tribocorrosion at OCP and the wear-accelerated corrosion. Based on the electrochemical technique and configuration proposed by Espallargas and coworkers [97], Licausi et al. (2015) [98] studied the tribocorrosion of Ti6Al4V biomedical alloy in artificial saliva at open circuit potential, measuring the galvanic potential and current between the wear track (anode) and the passive material (cathode). They could accurately simulate the current and potential during wear with the galvanic coupling model for tribocorrosion, which is based on the cathodic reaction kinetics (Figure 13).

Finally, a totally different configuration was used by Bryant et al. (2014) [99], who connected two working electrodes made of two different materials to investigate the galvanic coupling. They connected both electrodes through a ZRA, to measure the current flowing between the two materials. Galvanic coupling was found to significantly increase both pure wear and the wear-enhanced corrosion.

5. Standardized Tribocorrosion Test Produces

Although abrasion-corrosion and erosion-corrosion mechanisms of metals were described during the 1980s, no tribocorrosion mechanism in sliding contacts was proposed until the 1990s [3]. The tribocorrosion mechanisms have been evaluated through different approaches: synergistic, mechanistic, third-body, and nanochemical wear approaches [3]. In 1994, Madsen developed a standard guide to determine the synergism between wear and corrosion [6]. This is known as the synergistic approach, where the material loss is the sum of the material loss due to corrosion, the material loss due to wear, and a synergetic component. In order to assess some drawbacks of the synergistic approach collected in the ASTM G119 standard reported by some authors [3, 12, 13, 38], a test procedure based on the mechanistic approach was developed. According to this approach, the material loss due tribocorrosion is considered to be composed of two main contributions: anodic dissolution and mechanical removal of material. This test procedure was standardized in 2016 as a UNE 112086 standard [14]. The third-body approach in tribocorrosion was proposed by Mischler, et al. in 2001 [22], based on the third-body concept defined by Godet [100] in 1984 for dry sliding contacts. In this approach, the metal volume loss due to tribocorrosion is the sum of three contributions, namely, the mechanically detached material (abrasion, adhesion, or delamination), the chemically removed material (metal ions dissolved in the

electrolyte), and the metal oxidized to form the passive film. In turn, the metal particles in the track can be ejected from the contact, oxidized, or smeared and transferred to the metal surface. Finally, the most recent nanochemical wear approach considers subsurface deformation of the material in the contact under the mechanical solicitations. In dry sliding contacts, the plastic deformation leads to formation and movement of dislocations, leading to a recrystallization of the material and the modification of the mechanical behaviour in the contact [3, 101, 102]. In this section, the synergistic and mechanistic approaches collected in the ASMT G119 and UNE 112086 standards are explained in detail.

5.1. Wear and Corrosion Synergism Evaluation Procedure (ASTM G119). From approximately 1980 onwards, many researchers studied the synergism between wear and corrosion [4]. In 1981, Kim et al. (1981) [103] studied the synergism by examining the effect of load on the open circuit potential. It was found that wear increased the corrosion rate of passive materials, in environments and conditions in which the material loss due to pure corrosion was negligible in the absence of wear. The potential shifted to more active values and the current increased during sliding, indicating the increase in the kinetics of corrosion processes. Batchelor et al. (1988) [104] saw that the synergism of abrasion-corrosion was four times the corrosion rate even with negligible abrasion. Barker and Ball (1989) [105] observed that abrasion accelerated material degradation by removing the corrosion products or protective layer formed on top of the material and exposing the bare material to the corrosive environment. Kotlyar et al. (1988) [106] found that the magnitude of the synergistic effect between abrasion and corrosion was considerable, even when the influence of corrosion was small. Furthermore, they observed that the total abrasive-corrosive wear increased with increasing applied load, abrasive hardness, and decreasing solution pH. After several previous studies, Madsen [4, 107, 108] developed a standard guide in 1994 [6], to quantify the synergism between wear and corrosion. The ASTM standard consisted of four tests where the mechanical and electrochemical conditions were modified: corrosion only, wear only, and a combination of corrosion and wear.

According to the standard, the total material loss (T) corresponds to the total degradation due to wear and corrosion, i.e., tribocorrosion. The term includes the contributions from mechanical wear, corrosion dissolution, and the interaction between them and can be defined as follows:

$$T = W_0 + C_0 + S \tag{2}$$

with W_0 being the rate of material loss in the absence of corrosion, C_0 the electrochemical corrosion rate when no mechanical wear is applied, and S the synergetic component.

Since wear affects corrosion, and corrosion affects wear, the synergetic component can be further divided into two components, namely, the increase in the mechanical wear due to corrosion (ΔW_c) and the increase in corrosion due to mechanical wear (ΔC_w):

$$S = \Delta W_c + \Delta C_w, \tag{3}$$

where ΔW_c and ΔC_w can be calculated as follows:

$$\Delta W_c = W_c - W_0 \tag{4}$$

$$\Delta C_w = C_w - C_0 \tag{5}$$

with W_c being the total wear component of T and C_w the electrochemical corrosion during corrosive wear.

The above-mentioned parameters can be calculated, as specified in the ASTM G119 standard, as follows:

(i) T is material loss after a corrosion-wear test at open circuit potential.

(ii) W_0 can be obtained from the material loss after a wear test in the absence of corrosion. For this aim, the sample must be cathodically polarized one volt with respect to the free corrosion potential, so that corrosion is inhibited.

(iii) C_w is calculated from the corrosion current obtained in a potentiodynamic polarization test under mechanical wear, by using Faraday's law (Eq. (1)).

(iv) C_0 is calculated similarly to C_w from the corrosion current obtained from a potentiodynamic polarization test without mechanical wear.

Finally, the standard defines three dimensionless factors to describe the degree of wear-corrosion synergism:

(i) The total synergism factor: $\dfrac{T}{(T - S)}$ (6)

(ii) The corrosion augmentation factor: $\dfrac{(C_0 + \Delta C_w)}{C_0}$ (7)

(iii) The wear augmentation factor: $\dfrac{(W_0 + \Delta W_c)}{W_0}$ (8)

Figure 14 shows a graphic representation of the synergetic contributions of wear and corrosion on an AISI 304 stainless steel in seawater under different applied loads [30], obtained according to the ASTM G119 standard.

5.1.1. Tribocorrosion Studies Performed with the ASTM G119 Procedure. The ASTM G119 standard has been widely used to quantify the synergism of a large number of materials in different environments [33, 34, 109–117]. Neville and Hu (2001) [118] performed erosion-corrosion tests and observed that the resistance to material loss did not increase with the increase in hardness of the studied alloy, since corrosion was found to have an important synergistic effect on erosion. Following the Standard procedure, Gant et al. (2004) [119] obtained a synergistic component that was larger than the material loss due to pure corrosion and pure wear only, by an order of magnitude. Thakare et al. (2007) [120] performed abrasion-corrosion tests and obtained negative synergism. They attributed this effect to the surface chemistry modification effects such as passive film formation or depletion of most active surface compositions in contact with the electrolyte, which lowered abrasion due to corrosion. Lu et al. (2011) [121] investigated

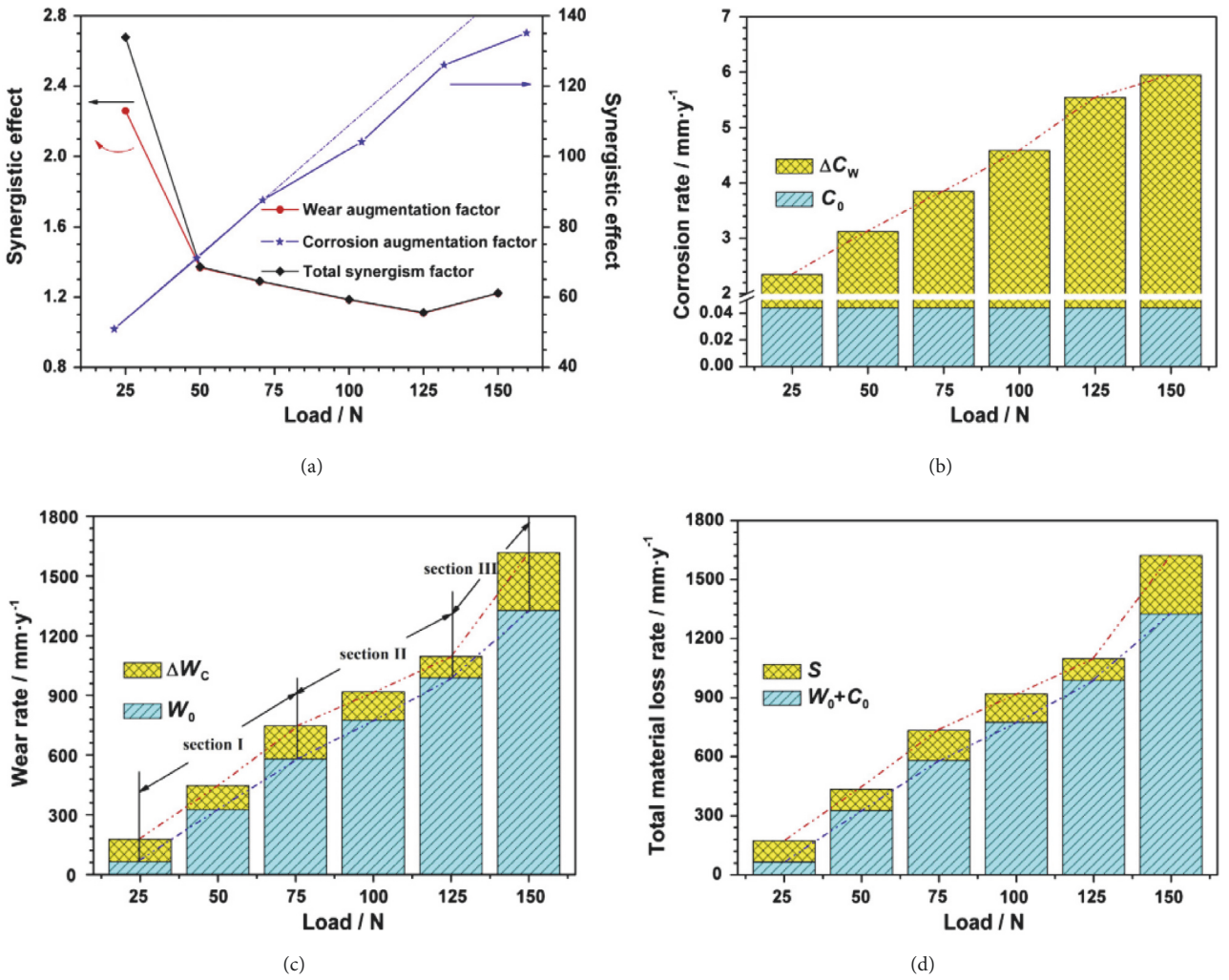

FIGURE 14: Synergetic contributions of mechanical wear and corrosion to each other and total material loss for a AISI 304 stainless steel at various applied loads in artificial seawater [30].

the synergism of mechanical and electrochemical factors in erosion-corrosion and observed that the synergism resulted mainly from corrosion-enhanced erosion. Yue Zhang et al. (2014) [30] investigated the influence of microstructure evolution on tribocorrosion of a 304 stainless steel, and the wear-corrosion synergistic degree was found to be dependent on the characteristics of microstructural evolution. Hardening of the steel due to plastic deformation, by both twinning and friction-induced martensite formation, led to enhanced wear resistance but, in turn, the galvanic corrosion of the thus-formed martensite led to a decrease in the surface hardness (corrosion-accelerated wear). Abedini and Ghasemi (2014) [122] performed erosion-corrosion tests and evaluated the synergism at different impingement angles. They observed that the higher rates corresponded to an angle of 40◦, and the total synergistic effect was mainly an effect of corrosion on erosion.

Several authors have used this protocol to build wear-corrosion maps, which helped to evaluate the influence of different variables. Bello et al. (2007) [123] investigated the synergistic effects of abrasion and corrosion and developed a mechanistic abrasion-corrosion map to establish the influence between abrasion and corrosion processes. Stack et al. (2011) [124] performed microabrasion corrosion tests to evaluate the effect of load and solution pH and constructed synergism maps showing transitions between microabrasion and corrosion regimes, as a function of load and solution pH.

5.2. Tribocorrosion Test Procedure for Passive Materials (UNE 112086:2016). In spite of growing interest and enhancement of electrochemical techniques, there was no standardized testing methodology for tribocorrosion evaluation until 2016. The only existing standard was the ASTM G119 [6], which describes a method to determine the synergism between wear and corrosion. However, different approaches were developed to evaluate the tribocorrosion behaviour of passive materials, in order to assess some drawbacks of the ASTM standard, reported by some authors [3, 12, 13, 38]. Based on the test procedures suggested by several researchers, a new standard was developed in 2016. The ASTM [6] standard involves wear

testing under anodic and cathodic polarization, whereas the new UNE 112086 [14] standard comprises wear tests at open circuit potential.

As reported by several authors [3, 12, 13, 38], the main shortcoming of the ASTM G119 standard is that the methodology employed does not separate measurements of the different contributions to the total material loss. According to the ASTM standard, material loss due to wear is obtained by performing sliding tests at cathodic potentials, where corrosion is negligible. However, the material loss measured does not necessarily represent the real conditions correctly since, in the absence of corrosion, the contribution of corrosion products to the mechanical response of the surface cannot be considered, as explained by Diomidis and coworkers [10, 12]. Furthermore, Akonko et al. (2005) [125] demonstrated that the wear volume depended on the cathodic potential selected and could vary by an order of magnitude due to the sensitivity to hydrogen embrittlement of the metal. On the other hand, the standard does not consider the galvanic couple generated between the worn and unworn areas during sliding either. Another considerable drawback, according to Diomidis et al. [10, 12], is that the standard does not provide information on the different processes that might take place in the different parts of the wear track, since it does not consider the different processes occurring within the wear track.

The protocol suggested in the UNE standard to assess the shortcomings of the ASTM standard can be used to identify and quantify the different mechanisms leading to material loss, i.e., mechanical and electrochemical mechanisms. Furthermore, it can also be used to identify the origin of material loss from different parts of the wear track, that is, from the active areas and partially or fully repassivated areas inside the track [3, 12, 13, 38].

The new approach consists of a series of successive steps during which essential data on tribocorrosion behaviour of materials is acquired:

(1) Open circuit potential registration until reaching a steady state

(2) Electrochemical impedance spectroscopy: after a stable potential is reached, an electrochemical impedance spectroscopy measurement is performed in OCP conditions. The polarization resistance (R_p) value obtained from this measurement is then used to calculate the corrosion current density (i_{pass}) of the passivated material as follows:

$$r_{pass} = R_p.A_0 \tag{9}$$

$$i_{pass} = \frac{B}{r_{pass}} \tag{10}$$

where r_{pass} is the specific polarization resistance of the passive material, A_0 the exposed surface area, and B a constant with typical values between 13 and 15 mV for metallic materials.

(3) First sliding wear test: the next step consists of determining the corrosion rate of the depassivated material inside the wear track. For this purpose, a sliding wear test should be performed in order to remove the passive layer and keep the material in the wear track in a continuous active state. The time between two successive contact events during sliding (t_{rot}) needs to be low enough to avoid passivation of the material in the wear track. The potential is registered during the sliding process, and the stable potential during sliding (E^s_{oc}) is calculated. This potential is a mixed potential resulting from the galvanic coupling of the active and passive areas.

(4) Second sliding wear test and second EIS - measurement: the effect of sliding on the corrosion resistance can be evaluated by performing an EIS measurement during sliding, once the sliding steady state has been achieved. In order to assure the stable state during sliding, some researchers have registered the EIS data by imposing a fixed potential on the system, which corresponds to the average potential value during sliding (E^s_{oc}) calculated in the previous step. The polarization resistance during sliding (R_{ps}) obtained is a combination of two polarization resistances, namely, the resistances corresponding to the active (R_{act}) and passive areas (R_{pass}):

$$\frac{1}{R_{ps}} = \frac{1}{R_{act}} + \frac{1}{R_{pass}} \tag{11}$$

$$R_{act} = \frac{r_{act}}{A_{act}} \tag{12}$$

$$R_{pass} = \frac{r_{pass}}{A_0 - A_{act}}. \tag{13}$$

Since r_{pass} is known from (9), r_{act} can be calculated as follows:

$$r_{act} = \frac{A_{tr}.R_{ps}.r_{pass}}{r_{pass-}R_{ps}.\left(A_0 - A_{act}\right)}. \tag{14}$$

The corrosion current density of the active material (i_{act}) can be obtained from the next equation:

$$i_{act} = \frac{B}{r_{act}}. \tag{15}$$

This test procedure can be used to quantify the reduction in the corrosion resistance of the studied material during sliding, by comparing the polarization resistances from the EIS data obtained before and during sliding.

The material loss due to corrosion in the wear track (W^c_{act}) can be calculated using Faraday's law:

$$W^c_{act} = i_{act}.A_{act}.\frac{M}{n.F.\rho}N.t_{lat}, \tag{16}$$

with M being the molecular weight, n the number of electrons involved in the anodic process, ρ the density, and F the Faraday constant (96500 C). N corresponds to the number

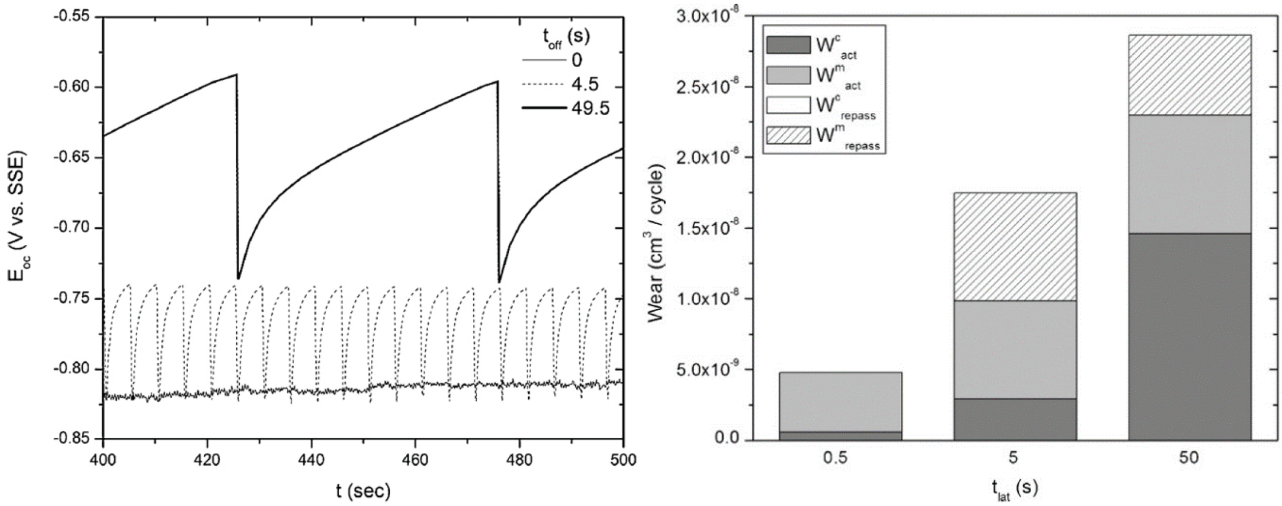

FIGURE 15: Left: evolution of continuous (t_{lat}=0) and intermittent (t_{lat}=4.5s and t_{lat}=49.5s) potential for an AISI 316 stainless steel in 0.5M H_2SO_4 at a rotation period (t_{rot}) of 0.5s. Right: contribution of the tribocorrosion components to the total volumetric material loss at the different latency times [13].

of cycles and t_{lat} is the latency time of the sliding test. The material loss due to wear and corrosion (W_{tr}) can be obtained from the volume of the wear track generated after the tribocorrosion test. Finally, the material loss due to mechanical wear in the wear track (W^m_{act}) can be calculated from the following equation:

$$W_{tr} = W^c_{act} + W^m_{act}. \tag{17}$$

In the case of intermittent sliding, W_{tr} is expressed as the sum of components related to both passive and active areas present in the wear track:

$$W_{tr} = W^c_{act} + W^m_{act} + W^c_{repass} + W^m_{repass} \tag{18}$$

with W^c_{repass} and W^m_{repass} being the material loss of the repassivated material in the wear track due to corrosion and mechanical wear, respectively. W^c_{repass} is calculated similarly to W^c_{act} in (16), but for the repassivated area

$$W^c_{repass} = i_{pass}.A_{repass}.\frac{M}{nF\rho}.N.t_{lat}. \tag{19}$$

Finally, W^m_{repass} is obtained from (18), once the other values are known.

5.2.1. Tribocorrosion Studies Performed with the UNE 112086 Procedure. In 2009, Diomidis et al. proposed a testing protocol [12] to assess the drawbacks of the preexisting ASTM standard. Several studies have been performed following this procedure, before it was standardized in 2016 (UNE 112086). In 2010, they investigated the tribocorrosion of an AISI 316 stainless steel in a diluted sulphuric acid solution [13]. They applied the protocol in order to determine the contributions of the different mechanical and corrosive components involved in material loss (Figure 15). They also quantified the synergism between wear and corrosion by calculating the corrosion current density from the polarization resistance values obtained in the impedance measurements. V. Saenz de Viteri et al. (2015) [126] studied the tribocorrosion behaviour of a Ti6Al4V alloy with several Ti-C-N coatings in simulated body fluids and found that the coating provided the system with improved performance against tribocorrosion and fretting. Lucia Mendizabal et al. (2015) [73] studied the tribocorrosion response of a multilayer TaN film deposited on titanium alloy in simulated body fluids. The corrosion resistance of the coatings was found to decrease during sliding, and the wear rate was observed to improve compared with the uncoated titanium alloy. Fatma Ben Saada et al. (2015) [127] investigated the tribocorrosion behaviour of an AISI 304L stainless steel in a mixture of olive pomace and tap water filtrate, by performing both continuous and intermittent sliding tests. They observed that the damage caused by tribocorrosion was more noticeable under intermittent sliding, due to the partially active state of the wear track, since it was constantly being passivated and repassivated. They [128] also studied the improvement of the tribocorrosion properties for the alloy by using severe shot peening.

6. Tribocorrosion Modelling

Development of theoretical models to predict the material loss due to the synergistic effect of wear and corrosion has been of great interest over the last two decades. However, the implication of different influencing parameters in tribocorrosion systems hinders the postulation of models. In 1998, Mischler et al. [129] developed a model to describe the effect of mechanical and material parameters on the wear-assisted corrosion rate of passive metals in two-body sliding contacts. They considered the effect of normal load and the passivation rate of the materials. Mischler et al. [129] and Landolt et al. [8] correlated the passivation charge density and the depassivation rate. Several models have been proposed

thenceforth, and some of the most recent ones are compiled in this section.

Jiang et al. (2002) [130] developed a model to describe interactions between wear and corrosion in sliding contacts. They incorporated different factors such as experimental and environmental conditions and material properties. In 2006, Jiang and Stack (2006) [131] proposed mechanisms for wear debris generation and validated the mathematical models which were developed, based on the proposed mechanisms. In 2010, von der Ohe et al. (2010) [132] developed a model to describe the multidegradation mechanism of tribocorrosion and static and cyclic fatigue taking place in a piston rod. In 2012, Papageorgiou and Mischler (2012) [133] suggested a quantitative galvanic coupling model that predicted potential evolution during tribocorrosion. Cao and coworkers developed [134] a predictive model considering the mechanical wear, wear-accelerated corrosion, and hydrodynamic lubrication applied to metal-on-metal implants. The model predictions were found to be consistent with tribocorrosion tests [135] and simulator results [136]. Recently, A. Dalmau et al. (2018) [137] developed a numerical contact model based on a Boundary Element Method (BEM) to describe the contact pressure distribution and quantification of the worn material as a function of time, taking into account the plastic behaviour of the material during the first cycles. They validated the model for a AISI 316L steel in a NaCl solution.

7. Conclusions and Future Perspective

A great number of studies have been carried out to assess the tribocorrosion behaviour of passive materials in order to get a closer insight into the mechanisms of this complex phenomenon. For this purpose, electrochemical techniques have been combined in different ways leading to several test procedures. This work compiles different test procedures and a combination of electrochemical techniques used by noteworthy researchers to assess tribocorrosion behaviour of passive materials. A brief explanation of the electrochemical techniques and studies made by tribocorrosion researchers has also been provided.

The early tribocorrosion studies were performed by combining potentiodynamic and potentiostatic polarization techniques, and they were focused on understanding the formation of the passive film and its behaviour under corrosion-wear solicitations. Other widely employed procedures combine open circuit potential and electrochemical impedance spectroscopy measurements. Electrochemical noise technique has been employed in more recent researches. Unlike polarization techniques, open circuit potential, and electrochemical impedance spectroscopy, no standard procedure has been developed by considering this technique so far. Electrochemical noise has been proven to be effective when evaluating tribocorrosion without externally disturbing the system. This technique provides information on both the corrosion potential and current variations taking place as a consequence of sliding. Besides, the configuration proposed by some researches [96–98] allows the worn and unworn areas to be physically separated. Hence, it could be interesting to run further analysis on the effectiveness of this technique with such a novel configuration and even standardize the procedure.

In the same vein, the standardization of an acceptable test procedure is a major concern for tribocorrosionists. Current standards can be used to characterise and evaluate tribocorrosion of passive materials, but there are still several drawbacks that have drawn criticism and disagreement among experts in the field. Until 2016, the only existing standard for tribocorrosion tests was the ASTM G119, which can be used to appraise the synergism between wear and corrosion. The synergistic approach focuses on the dependence of wear and corrosion but does not provide information on the nature of the interactions. A mechanistic approach was developed to overcome these shortcomings, and the test procedure was standardized in 2016. The UNE 112086 standard can be used to evaluate the combined action of wear and corrosion, taking into consideration the galvanic couple generated between the worn and unworn areas. This approach quantifies the mechanical and electrochemical contributions to material loss. However, there is no direct way to determine the mechanical contribution to material loss in the track, and it has commonly been calculated by subtracting the chemical contribution to the total material loss, as specified in (17). In turn, the selection of the oxidation state (n number) in (16) to calculate the chemical contribution has been found to affect the results considerably [8, 18, 21, 89]. In cases where the valence of oxidation products varies with the applied potential or for alloys, the value of n is uncertain, and detailed surface analysis such as X-ray photoelectron spectroscopy should be employed to determine it [3]. On the other hand, wear and corrosion are not independent processes, although they interact with each other, and calculating these two contributions alone is not enough to describe the tribocorrosion process in sliding contacts. Generation of the third-body particles and their effect during rubbing must be considered, since they play an important role. This debris can aggravate the extent of wear by acting as abrasives, or they can form a lubricating layer reducing the friction [8, 9, 17–19]. In this regard, the third-body approach considers the behaviour of these particles in the contact, but no understanding on the formation, transformation, and ejection is provided [3]. Finally, the microstructural transformations taking place in the contacts under the applied mechanical solicitations should also been considered, as proposed in the nanochemical wear approach. Therefore, one of the most significant challenges in the field is developing a more accurate tribocorrosion mechanism that considers all the aspects mentioned above that could allow the phenomenon to be predicted. Furthermore, the need for standardized test equipment is also a drawback in the advance of the knowledge generation process, since the lack of a reliable apparatus leads to discrepancies in the results and how they are interpreted.

Another challenge in the study of tribocorrosion to be addressed is adapting test procedures for passive materials to assessment of tribocorrosion in active materials. Unlike passive materials, active materials do not generate a protective oxide layer on the surface when in contact with a

corrosive media. On the contrary, the oxide layer in the surface is rather porous with low adherence. Therefore, the material loss is a consequence not only of wear and corrosion processes taking place in the wear track, but also of pure corrosion in the unworn surface. Tribocorrosion of passive materials has been widely studied, whereas the response of active materials is less documented. Recently, A. López et al. (2015) [138] studied the tribocorrosion behaviour of High-Strength Low-Alloyed (HSLA) steels in synthetic seawater by means of potentiodynamic and potentiostatic polarization techniques and evaluated the wear-corrosion synergism according to the ASTM G119 standard. In a following study, A. López-Ortega et al. (2018) [139] evaluated the effect of temperature on the tribocorrosion of HSLA steels in synthetic seawater, using a test protocol based on the UNE 112086 standard. The results showed that, unlike the observation for passive materials, sliding resulted in a potential shift towards more positive values and a current shift to more negative values. The material in the wear track was found to be more cathodic than the unworn surface, and thus, the galvanic couple generated between worn and unworn areas promoted the corrosion of the unworn surface. This opposing behaviour of active materials compared to passive alloys demonstrates the need to develop a test protocol to evaluate the tribocorrosion behaviour of active materials. Furthermore, since the unworn area is actively corroding during immersion tests, the methods currently used to quantify mechanical and electrochemical process contributions to the total material loss in passive materials are not appropriate. A closer understanding on the tribocorrosion degradation mechanism of active metals and alloys could provide better awareness of the use of these materials, with or without protective coatings, in order to enlarge their useful life in applications where passive materials are not suitable for use, i.e., higher costs and lower mechanical properties.

Conflicts of Interest

The authors declare that they have no conflicts of interest.

Acknowledgments

The authors would like to acknowledge the FRONTIERS III project (ELKARTEK 2017, KK-2017/00096) financed by the Basque Country. The authors would also like to acknowledge the Education, Linguistic Politics and Culture Department of the Basque Government for its support through the "*Programa Predoctoral de Formación de Personal Investigador No Doctor (PRE_2017_2_0088)*" grant awarded to the primary author.

References

[1] ASTM G40-17, *Standard Terminology Relating to Wear and Erosion*, ASTM International, West Conshohocken, PA, USA, 2017.

[2] M. T. Mathew, P. Srinivasa Pai, R. Pourzal, A. Fischer, and M. A. Wimmer, "Significance of Tribocorrosion in Biomedical Applications: Overview and Current Status," *Advances in Tribology*, vol. 2009, Article ID 250986, pp. 1–12, 2009.

[3] D. Landolt and S. Mischler, *Tribocorrosion of Passive Metals and Coatings*, ISBN: 978-1-84569-966-6, Woodhead Publishing, Cambridge, UK, 2011.

[4] S. W. Watson, F. J. Friedersdorf, B. W. Madsen, and S. D. Cramer, "Methods of measuring wear-corrosion synergism," *Wear*, vol. 181–183, no. 2, pp. 476–484, 1995.

[5] S. Mischler, E. A. Rosset, and D. Landolt, "Effect of Corrosion on the Wear Behavior of Passivating Metals in Aqueous Solutions," *Tribology and Interface Engineering Series*, vol. 25, no. C, pp. 245–253, 1993.

[6] G119-09 ASTM, *Standard Guide for Determining Synergism Between Wear and Corrosio*, ASTM International, West Conshohocken, PA, USA, 2016.

[7] D. Landolt, "Electrochemical and materials aspects of tribocorrosion systems," *Journal of Physics D: Applied Physics*, vol. 39, no. 15, article no. S01, pp. 3121–3127, 2006.

[8] D. Landolt, S. Mischler, and M. Stemp, "Electrochemical methods in tribocorrosion: A critical appraisal," *Electrochimica Acta*, vol. 46, no. 24-25, pp. 3913–3929, 2001.

[9] G. Stachowiak, M. Salasi, and G. Stachowiak, "Three-Body Abrasion Corrosion Studies of High-Cr Cast Irons: Benefits and Limitations of Tribo-electrochemical Methods," *Journal of Bio- and Tribo-Corrosion*, vol. 1, no. 1, article no. 6, 2015.

[10] J.-P. Celis and P-. Ponthiaux, *Testing Tribocorrosion of Passivating Materials Supporting Research and Industrial Innovation*, ISBN: 978-1-907975-20-2, Handbook. Maney Publishing, UK, 2012.

[11] S. Mischler, "Triboelectrochemical techniques and interpretation methods in tribocorrosion: A comparative evaluation," *Tribology International*, vol. 41, no. 7, pp. 573–583, 2008.

[12] N. Diomidis, J.-P. Celis, P. Ponthiaux, and F. Wenger, "A methodology for the assessment of the tribocorrosion of passivating metallic materials," *Lubrication Science*, vol. 21, no. 2, pp. 53–67, 2009.

[13] N. Diomidis, J.-P. Celis, P. Ponthiaux, and F. Wenger, "Tribocorrosion of stainless steel in sulfuric acid: Identification of corrosion-wear components and effect of contact area," *Wear*, vol. 269, no. 1-2, pp. 93–103, 2010.

[14] UNE 112086:2016, Ensayos de tribocorrosión en materiales pasivos, 07 September 2016.

[15] H. Shih, *Corrosion Resistance*, ISBN 978-953-51-0467-4, InTech, 2012.

[16] S. Mischler and P. Ponthiaux, "A round robin on combined electrochemical and friction tests on alumina/stainless steel contacts in sulphuric acid," *Wear*, vol. 248, no. 1-2, pp. 211–225, 2001.

[17] R. I. Trezona, D. N. Allsopp, and I. M. Hutchings, "Transitions between two-body and three-body abrasive wear: Influence of test conditions in the microscale abrasive wear test," *Wear*, vol. 225-229, no. I, pp. 205–214, 1999.

[18] D. Landolt, S. Mischler, M. Stemp, and S. Barril, "Third body effects and material fluxes in tribocorrosion systems involving a sliding contact," *Wear*, vol. 256, no. 5, pp. 517–524, 2004.

[19] N. Diomidis and S. Mischler, "Third body effects on friction and wear during fretting of steel contacts," *Tribology International*, vol. 44, no. 11, pp. 1452–1460, 2011.

[20] P. Ponthiaux, F. Wenger, D. Drees, and J. P. Celis, "Electrochemical techniques for studying tribocorrosion processes," *Wear*, vol. 256, no. 5, pp. 459–468, 2004.

[21] M. Stemps, S. Mischler, and D. Landolt, "The effect of contact configuration on the tribocorrosion of stainless steel in reciprocating sliding under potentiostatic control," *Corrosion Science*, vol. 45, no. 3, pp. 625–640, 2003.

[22] S. Mischler, A. Spiegel, M. Stemp, and D. Landolt, "Influence of passivity on the tribocorrosion of carbon steel in aqueous solutions," *Wear*, vol. 250-251, no. 2, pp. 1295–1307, 2001.

[23] P. Jemmely, S. Mischler, and D. Landolt, "Electrochemical modeling of passivation phenomena in tribocorrosion," *Wear*, vol. 237, no. 1, pp. 63–76, 2000.

[24] Y. Sun and V. Rana, "Tribocorrosion behaviour of AISI 304 stainless steel in 0.5 M NaCl solution," *Materials Chemistry and Physics*, vol. 129, no. 1-2, pp. 138–147, 2011.

[25] X. Y. Wang and D. Y. Li, "Application of an electrochemical scratch technique to evaluate contributions of mechanical and electrochemical attacks to corrosive wear of materials," *Wear*, vol. 259, no. 7-12, pp. 1490–1496, 2005.

[26] Y. Sun and R. Bailey, "Improvement in tribocorrosion behavior of 304 stainless steel by surface mechanical attrition treatment," *Surface and Coatings Technology*, vol. 253, pp. 284–291, 2014.

[27] R. Pileggi, M. Tului, D. Stocchi, and S. Lionetti, "Tribocorrosion behaviour of chromium carbide based coatings deposited by HVOF," *Surface and Coatings Technology*, vol. 268, pp. 247–251, 2015.

[28] A. C. Vieira, A. R. Ribeiro, L. A. Rocha, and J. P. Celis, "Influence of pH and corrosion inhibitors on the tribocorrosion of titanium in artificial saliva," *Wear*, vol. 261, no. 9, pp. 994–1001, 2006.

[29] J. Chen, J. Wang, F. Yan, Q. Zhang, and Q.-A. Li, "Effect of applied potential on the tribocorrosion behaviors of Monel K500 alloy in artificial seawater," *Tribology International*, vol. 81, pp. 1–8, 2015.

[30] Y. Zhang, X. Yin, J. Wang, and F. Yan, "Influence of microstructure evolution on tribocorrosion of 304SS in artificial seawater," *Corrosion Science*, vol. 88, pp. 423–433, 2014.

[31] J. Chen and F.-Y. Yan, "Tribocorrosion behaviors of Ti-6Al-4V and Monel K500 alloys sliding against 316 stainless steel in artificial seawater," *Transactions of Nonferrous Metals Society of China*, vol. 22, no. 6, pp. 1356–1365, 2012.

[32] J. Chen, Q. Zhang, Q. Li, S. Fu, and J. Wang, "Corrosion and tribocorrosion behaviors of AISI 316 stainless steel and Ti6Al4V alloys in artificial seawater," *Transactions of Nonferrous Metals Society of China*, vol. 24, no. 4, pp. 1022–1031, 2014.

[33] Y. Zhang, X. Yin, and F. Yan, "Effect of halide concentration on tribocorrosion behaviour of 304SS in artificial seawater," *Corrosion Science*, vol. 99, pp. 272–280, 2015.

[34] Y. Zhang, X.-Y. Yin, and F.-Y. Yan, "Tribocorrosion behaviour of type S31254 steel in seawater: Identification of corrosion-wear components and effect of potential," *Materials Chemistry and Physics*, vol. 179, pp. 273–281, 2016.

[35] Y. Sun and E. Haruman, "Tribocorrosion behaviour of low temperature plasma carburised 316L stainless steel in 0.5M NaCl solution," *Corrosion Science*, vol. 53, no. 12, pp. 4131–4140, 2011.

[36] B. A. Obadele, M. L. Lepule, A. Andrews, and P. A. Olubambi, "Tribocorrosion characteristics of laser deposited Ti-Ni-ZrO2 composite coatings on AISI 316 stainless steel," *Tribology International*, vol. 78, pp. 160–167, 2014.

[37] A. C. Vieira, L. A. Rocha, N. Papageorgiou, and S. Mischler, "Mechanical and electrochemical deterioration mechanisms in the tribocorrosion of Al alloys in NaCl and in NaNO3 solutions," *Corrosion Science*, vol. 54, no. 1, pp. 26–35, 2012.

[38] Y. Yu, *Bio-Tribocorrosion in Biomaterials and Medical Implants*, ISBN: 978-0-85709-540-4, Woodhead Publishing, 2013.

[39] M. Azzi and J. A. Szpunar, "Tribo-electrochemical technique for studying tribocorrosion behavior of biomaterials," *Biomolecular Engineering*, vol. 24, no. 5, pp. 443–446, 2007.

[40] A. de Frutos Rozas, *Tribocorrosión de biomateriales metálicos modificados superficialmente mediante técnicas de vacío [Ph.D. thesis]*, Universidad Autónoma de Madrid, Facultad de Ciencias, June 2010.

[41] X. Luo, X. Li, Y. Sun, and H. Dong, "Tribocorrosion behavior of S-phase surface engineered medical grade Co-Cr alloy," *Wear*, vol. 302, no. 1-2, pp. 1615–1623, 2013.

[42] Z. Guo, X. Pang, Y. Yan, K. Gao, A. A. Volinsky, and T.-Y. Zhang, "CoCrMo alloy for orthopedic implant application enhanced corrosion and tribocorrosion properties by nitrogen ion implantation," *Applied Surface Science*, vol. 347, Article ID 30147, pp. 23–34, 2015.

[43] A. M. Ribeiro, A. C. Alves, L. A. Rocha, F. S. Silva, and F. Toptan, "Synergism between corrosion and wear on CoCrMo-Al2O3 biocomposites in a physiological solution," *Tribology International*, vol. 91, 2017.

[44] Z. Doni, A. C. Alves, F. Toptan et al., "Dry sliding and tribocorrosion behaviour of hot pressed CoCrMo biomedical alloy as compared with the cast CoCrMo and Ti6Al4V alloys," *Materials and Corrosion*, vol. 52, pp. 47–57, 2013.

[45] V. G. Pina, A. Dalmau, F. Devesa, V. Amigó, and A. I. Muñoz, "Tribocorrosion behavior of beta titanium biomedical alloys in phosphate buffer saline solution," *Journal of the Mechanical Behavior of Biomedical Materials*, vol. 46, pp. 59–68, 2015.

[46] I. Hacisalihoglu, A. Samancioglu, F. Yildiz, G. Purcek, and A. Alsaran, "Tribocorrosion properties of different type titanium alloys in simulated body fluid," *Wear*, vol. 332-333, 2016.

[47] R. Baboian, Ed., *ASTM corrosion tests and standards*, ISBN: 0-8031-2098-2, ASTM International, 2013.

[48] A. Igual Muñoz and L. Casabán Julián, "Influence of electrochemical potential on the tribocorrosion behaviour of high carbon CoCrMo biomedical alloy in simulated body fluids by electrochemical impedance spectroscopy," *Electrochimica Acta*, vol. 55, no. 19, pp. 5428–5439, 2010.

[49] S. Mischler, A. Spiegel, and D. Landolt, "The role of passive oxide films on the degradation of steel in tribocorrosion systems," *Wear*, vol. 225-229, no. II, pp. 1078–1087, 1999.

[50] P. Ponthiaux, F. Wenger, and J.-P. Celis, "Tribocorrosion: Material Behavior Under Combined Conditions of Corrosion and Mechanical Loading, Corrosion Resistance," in *In Tech*, Dr. Shih, Ed., ISBN: 978-953-51-0467-4, 2012, http://dx.doi.org/10.5772/35634.

[51] ASTM G102-89(2015)e1, *Standard Practice for Calculation of Corrosion Rates and Related Information from Electrochemical Measurements*, ASTM International, West Conshohocken, PA, USA, 2015.

[52] I. García, D. Drees, and J. P. Celis, "Corrosion-wear of passivating materials in sliding contacts based on a concept of active wear track area," *Wear*, vol. 249, no. 5-6, pp. 452–460, 2001.

[53] M. Stemp, S. Mischler, and D. Landolt, "The effect of mechanical and electrochemical parameters on the tribocorrosion rate of stainless steel in sulphuric acid," *Wear*, vol. 255, no. 1-6, pp. 466–475, 2003.

[54] S. Barril, S. Mischler, and D. Landolt, "Electrochemical effects on the fretting corrosion behaviour of Ti6Al4V in 0.9% sodium chloride solution," *Wear*, vol. 259, no. 1-6, pp. 282–291, 2005.

[55] M. Favero, P. Stadelmann, and S. Mischler, "Effect of the applied potential of the near surface microstructure of a 316L steel submitted to tribocorrosion in sulfuric acid," *Journal of Physics D: Applied Physics*, vol. 39, no. 15, article no. S07, pp. 3175–3183, 2006.

[56] J. Stojadinović, D. Bouvet, M. Declercq, and S. Mischler, "Effect of electrode potential on the tribocorrosion of tungsten," *Tribology International*, vol. 42, no. 4, pp. 575–583, 2009.

[57] A. Bidiville, M. Favero, P. Stadelmann, and S. Mischler, "Effect of surface chemistry on the mechanical response of metals in sliding tribocorrosion systems," *Wear*, vol. 263, no. 1-6, pp. 207–217, 2007.

[58] M. N. F. Ismail, T. J. Harvey, J. A. Wharton, R. J. K. Wood, and A. Humphreys, "Surface potential effects on friction and abrasion of sliding contacts lubricated by aqueous solutions," *Wear*, vol. 267, no. 11, pp. 1978–1986, 2009.

[59] N. Espallargas and S. Mischler, "Tribocorrosion behaviour of overlay welded Ni-Cr 625 alloy in sulphuric and nitric acids: Electrochemical and chemical effects," *Tribology International*, vol. 43, no. 7, pp. 1209–1217, 2010.

[60] I. Golvano, I. Garcia, A. Conde, W. Tato, and A. Aginagalde, "Influence of fluoride content and pH on corrosion and tribocorrosion behaviour of Ti13Nb13Zr alloy in oral environment," *Journal of the Mechanical Behavior of Biomedical Materials*, vol. 49, pp. 186–196, 2015.

[61] S. Radice and S. Mischler, "Effect of electrochemical and mechanical parameters on the lubrication behaviour of Al2O3 nanoparticles in aqueous suspensions," *Wear*, vol. 261, no. 9, pp. 1032–1041, 2006.

[62] K. L. Dahm, "Direct observation of the interface during sliding tribo-corrosion," *Tribology International*, vol. 40, no. 10-12, pp. 1561–1567, 2007.

[63] N. Espallargas, C. Torres, and A. I. Muñoz, "A metal ion release study of CoCrMo exposed to corrosion and tribocorrosion conditions in simulated body fluids," *Wear*, vol. 332-333, 2017.

[64] Y. Liao, E. Hoffman, M. Wimmer, A. Fischer, J. Jacobs, and L. Marks, "CoCrMo metal-on-metal hip replacements," *Physical Chemistry Chemical Physics*, vol. 15, no. 3, pp. 746–756, 2013.

[65] S. Hiromoto and S. Mischler, "The influence of proteins on the fretting-corrosion behaviour of a Ti6Al4V alloy," *Wear*, vol. 261, no. 9, pp. 1002–1011, 2006.

[66] M. T. Mathew, M. J. Runa, M. Laurent, J. J. Jacobs, L. A. Rocha, and M. A. Wimmer, "Tribocorrosion behavior of CoCrMo alloy for hip prosthesis as a function of loads: A comparison between two testing systems," *Wear*, vol. 271, no. 9-10, pp. 1210–1219, 2011.

[67] K. Sadiq, M. M. Stack, and R. A. Black, "Wear mapping of CoCrMo alloy in simulated bio-tribocorrosion conditions of a hip prosthesis bearing in calf serum solution," *Materials Science and Engineering C: Materials for Biological Applications*, vol. 49, pp. 452–462, 2015.

[68] M. J. Runa, M. T. Mathew, and L. A. Rocha, "Tribocorrosion response of the Ti6Al4V alloys commonly used in femoral stems," *Tribology International*, vol. 68, pp. 85–93, 2013.

[69] R. Bayón, A. Igartua, J. J. González, and U. Ruiz De Gopegui, "Influence of the carbon content on the corrosion and tribocorrosion performance of Ti-DLC coatings for biomedical alloys," *Tribology International*, vol. 88, article no. 3593, pp. 115–125, 2015.

[70] S-I.. Pyun, H-C. Shin, J-W. Lee, and J-Y. Go, "Electrochemistry of Insertion Materials for Hydrogen and Lithium," in *Chapter 2: Electrochemical Methods*, ISBN: 978-3-642-29463-1, pp. 11–32, Springer, 2012.

[71] A. Lasia, *Electrochemical Impedance Spectroscopy and its Applications*, ISBN: 978-1-4614-8932-0, Springer, 2014.

[72] F. Scholz, *Electroanalytical Methods, Guide to Experiments and Applications*, Springer, Guide to Experiments and Applications, 2010.

[73] L. Mendizabal, A. Lopez, R. Bayón, P. Herrero-Fernandez, J. Barriga, and J. J. Gonzalez, "Tribocorrosion response in biological environments of multilayer TaN films deposited by HPPMS," *Surface and Coatings Technology*, vol. 295, pp. 60–69, 2015.

[74] R. Bayón, A. Igartua, X. Fernández et al., "Corrosion-wear behaviour of PVD Cr/CrN multilayer coatings for gear applications," *Tribology International*, vol. 42, no. 4, pp. 591–599, 2009.

[75] M. J. Runa, M. T. Mathew, M. H. Fernandes, and L. A. Rocha, "First insight on the impact of an osteoblastic layer on the bio-tribocorrosion performance of Ti6Al4V hip implants," *Acta Biomaterialia*, vol. 12, no. 1, pp. 341–351, 2015.

[76] V. S. De Viteri, R. Bayón, A. Igartua et al., "Structure, tribocorrosion and biocide characterization of Ca, P and I containing TiO2 coatings developed by plasma electrolytic oxidation," *Applied Surface Science*, vol. 367, pp. 1–10, 2016.

[77] N. Papageorgiou, A. Von Bonin, and N. Espallargas, "Tribocorrosion mechanisms of NiCrMo-625 alloy: An electrochemical modeling approach," *Tribology International*, vol. 73, pp. 177–186, 2014.

[78] B. Alemón, M. Flores, W. Ramírez, J. C. Huegel, and E. Broitman, "Tribocorrosion behavior and ions release of CoCrMo alloy coated with a TiAlVCN/CNx multilayer in simulated body fluid plus bovine serum albumin," *Tribology International*, vol. 81, pp. 159–168, 2015.

[79] M. Fazel, H. R. Salimijazi, M. A. Golozar, and M. R. Garsivaz Jazi, "A comparison of corrosion, tribocorrosion and electrochemical impedance properties of pure Ti and Ti6Al4V alloy treated by micro-arc oxidation process," *Applied Surface Science*, vol. 324, pp. 751–756, 2015.

[80] S. Rossi, L. Fedrizzi, M. Leoni, P. Scardi, and Y. Massiani, "(Ti,Cr)N and Ti/TiN PVD coatings on 304 stainless steel substrates: Wear-corrosion behaviour," *Thin Solid Films*, vol. 350, no. 1, pp. 161–167, 1999.

[81] S. A. Alves, R. Bayón, V. S. de Viteri et al., "Tribocorrosion Behavior of Calcium- and Phosphorous-Enriched Titanium Oxide Films and Study of Osteoblast Interactions for Dental Implants," *Journal of Bio- and Tribo-Corrosion*, vol. 1, no. 3, article no. 23, 2015.

[82] M. Buciumeanu, A. Bagheri, J. C. M. Souza, F. S. Silva, and B. Henriques, "Tribocorrosion behavior of hot pressed CoCrMo alloys in artificial saliva," *Tribology International*, vol. 97, pp. 423–430, 2016.

[83] Consejo Superior de Investigaciones Científicas (CSIC). Ciencia e ingeniería de la superficie de los materiales metálicos. Raycar (2000). ISBN: 84-00-07920-5.

[84] J. Botana Pedemonte, M. Marcos Bárcena, A. Aballe Villero. Ruido electroquímico: Métodos de análisis. Septem Ediciones (2002) ISBN: 84-95687-33-X.

[85] J. M. Sánchez-Amaya, M. Bethencourt, L. Gonzalez-Rovira, and F. J. Botana, "Medida de ruido electroquímico para el estudio de procesos de corrosión de aleaciones metálicas," *Revista de Metalurgia*, vol. 45, no. 2, pp. 142–156, 2009.

[86] P.-Q. Wu and J.-P. Celis, "Electrochemical noise measurements on stainless steel during corrosion-wear in sliding contacts," *Wear*, vol. 256, no. 5, pp. 480–490, 2004.

[87] R. J. K. Wood, J. A. Wharton, A. J. Speyer, and K. S. Tan, "Investigation of erosion-corrosion processes using electrochemical noise measurements," *Tribology International*, vol. 35, no. 10, pp. 631–641, 2002.

[88] F. Galliano, E. Galvanetto, S. Mischler, and D. Landolt, "Tribocorrosion behavior of plasma nitrided Ti-6Al-4V alloy in neutral NaCl solution," *Surface and Coatings Technology*, vol. 145, no. 1-3, pp. 121–131, 2001.

[89] A. de Frutos, M. A. Arenas, G. G. Fuentes et al., "Tribocorrosion behaviour of duplex surface treated AISI 304 stainless steel," *Surface and Coatings Technology*, vol. 204, no. 9-10, pp. 1623–1630, 2010.

[90] M. Salasi, G. Stachowiak, and G. Stachowiak, "Tribo-electrochemical behaviour of 316L stainless steel: The effects of contact configuration, tangential speed, and wear mechanism," *Corrosion Science*, vol. 98, pp. 20–32, 2015.

[91] A. K. Basak, P. Matteazzi, M. Vardavoulias, and J.-P. Celis, "Corrosion-wear behaviour of thermal sprayed nanostructured FeCu/WC-Co coatings," *Wear*, vol. 261, no. 9, pp. 1042–1050, 2006.

[92] J. de Damborenea, C. Navas, J. A. García, M. A. Arenas, and A. Conde, "Corrosion-erosion of TiN-PVD coatings in collagen and cellulose meat casing," *Surface and Coatings Technology*, vol. 201, no. 12, pp. 5751–5757, 2007.

[93] E. Gracia-Escosa, I. García, J. C. Sánchez-López et al., "Tribocorrosion behavior of TiBxCy/a-C nanocomposite coating in strong oxidant disinfectant solutions," *Surface and Coatings Technology*, vol. 263, pp. 78–85, 2015.

[94] Z. Quan, P.-Q. Wu, L. Tang, and J.-P. Celis, "Corrosion-wear monitoring of TiN coated AISI 316 stainless steel by electrochemical noise measurements," *Applied Surface Science*, vol. 253, no. 3, pp. 1194–1197, 2006.

[95] A. Berradja, F. Bratu, L. Benea, G. Willems, and J.-P. Celis, "Effect of sliding wear on tribocorrosion behaviour of stainless steels in a Ringer's solution," *Wear*, vol. 261, no. 9, pp. 987–993, 2006.

[96] R. C. C. Silva, R. P. Nogueira, and I. N. Bastos, "Tribocorrosion of UNS S32750 in chloride medium: Effect of the load level," *Electrochimica Acta*, vol. 56, no. 24, pp. 8839–8845, 2011.

[97] N. Espallargas, R. Johnsen, C. Torres, and A. I. Muñoz, "A new experimental technique for quantifying the galvanic coupling effects on stainless steel during tribocorrosion under equilibrium conditions," *Wear*, vol. 307, no. 1-2, pp. 190–197, 2013.

[98] M. P. Licausi, A. I. Muñoz, V. A. Borrás, and N. Espallargas, "Tribocorrosion Mechanisms of Ti6Al4V in Artificial Saliva by Zero-Resistance Ammetry (ZRA) Technique," *Journal of Bio- and Tribo-Corrosion*, vol. 1, no. 1, article no. 8, 2015.

[99] M. Bryant, R. Farrar, R. Freeman, K. Brummitt, J. Nolan, and A. Neville, "Galvanically enhanced fretting-crevice corrosion of cemented femoral stems," *Journal of the Mechanical Behavior of Biomedical Materials*, vol. 40, pp. 275–286, 2014.

[100] M. Godet, "The third-body approach: A mechanical view of wear," *Wear*, vol. 100, no. 1-3, pp. 437–452, 1984.

[101] J.-P. Celis, P. Ponthiaux, and F. Wenger, "Tribo-corrosion of materials: Interplay between chemical, electrochemical, and mechanical reactivity of surfaces," *Wear*, vol. 261, no. 9, pp. 939–946, 2006.

[102] D. Shakhvorostov, B. Gleising, R. Büscher, W. Dudzinski, A. Fischer, and M. Scherge, "Microstructure of tribologically induced nanolayers produced at ultra-low wear rates," *Wear*, vol. 263, no. 7-12, pp. 1259–1265, 2007.

[103] K. Y. Kim, V. Agarwala, and S. Bhattacharyya, "An electrochemical polarization technique for evaluation of wear-corrosion in moving components under stress," in *Wear of materials*, Ludema, Ed., pp. 772–778, ASME, New York, 1981.

[104] A. W. Batchelor and G. W. Stachowiak, "Predicting synergism between corrosion and abrasive wear," *Wear*, vol. 123, no. 3, pp. 281–291, 1988.

[105] K. C. Barker and A. Ball, "Synergistic abrasive-corrosive wear of chromium containing steels," *British Corrosion Journal*, vol. 24, no. 3, pp. 222–228, 1989.

[106] D. Kotlyar, C. H. Pitt, and M. E. Wadsworth, "Simultaneous corrosion and abrasion measurements under grinding conditions," *Corrosion*, vol. 44, no. 4, pp. 221–228, 1988.

[107] B. W. Madsen, "Measurement of wear and corrosion rates using a novel slurry wear test," *Materials Performance*, vol. 26, no. 1, pp. 21–28, 1987.

[108] B. W. Madsen, "Measurement of erosion-corrosion synergism with a slurry wear test apparatus," *Wear*, vol. 123, no. 2, pp. 127–142, 1988.

[109] S. Yin and D. Y. Li, "Effects of prior cold work on corrosion and corrosive wear of copper in HNO3 and NaCl solutions," *Materials Science and Engineering: A Structural Materials: Properties, Microstructure and Processing*, vol. 394, no. 1-2, pp. 266–276, 2005.

[110] S. Yin, D. Y. Li, and R. Bouchard, "Effects of the strain rate of prior deformation on the wear-corrosion synergy of carbon steel," *Wear*, vol. 263, no. 1-6, pp. 801–807, 2007.

[111] M. S. Jellesen, T. L. Christiansen, L. R. Hilbert, and P. Møller, "Erosion-corrosion and corrosion properties of DLC coated low temperature gas-nitrided austenitic stainless steel," *Wear*, vol. 267, no. 9-10, pp. 1709–1714, 2009.

[112] D. López, N. Alonso Falleiros, and A. Paulo Tschiptschin, "Effect of nitrogen on the corrosionerosion synergism in an austenitic stainless steel," *Tribology International*, vol. 44, no. 5, pp. 610–616, 2011.

[113] J. A. Alegría-Ortega, L. M. Ocampo-Carmona, F. A. Suárez-Bustamante, and J. J. Olaya-Flórez, "Erosion-corrosion wear of Cr/CrN multi-layer coating deposited on AISI-304 stainless steel using the unbalanced magnetron (UBM) sputtering system," *Wear*, vol. 290-291, pp. 149–153, 2012.

[114] Ç. Albayrak, I. Hacisalihoğlu, S. Yenal vangölü, and A. Alsaran, "Tribocorrosion behavior of duplex treated pure titanium in Simulated Body Fluid," *Wear*, vol. 302, no. 1-2, pp. 1642–1648, 2013.

[115] R. Priya, C. Mallika, and U. K. Mudali, "Wear and tribocorrosion behaviour of 304L SS, Zr-702, Zircaloy-4 and Ti-grade2," *Wear*, vol. 310, no. 1-2, pp. 90–100, 2014.

[116] C. T. Kwok, P. K. Wong, and H. C. Man, "Laser surface alloying of copper with titanium: Part I. Electrical wear resistance in dry condition. Part II. Electrical wear resistance in wet and corrosive condition," *Surface and Coatings Technology*, vol. 297, pp. 58–73, 2016.

[117] F. Ma, J. Li, Z. Zeng, and Y. Gao, "Structural, mechanical and tribocorrosion behaviour in artificial seawater of CrN/AlN nano-multilayer coatings on F690 steel substrates," *Applied Surface Science*, vol. 428, pp. 404–414, 2018.

[118] A. Neville and X. Hu, "Mechanical and electochemical interactions during liquid-solid impingement on high-alloy stainless steels," *Wear*, vol. 250-251, no. 2, pp. 1284–1294, 2001.

[119] A. J. Gant, M. G. Gee, and A. T. May, "The evaluation of tribo-corrosion synergy for WC-Co hardmetals in low stress abrasion," *Wear*, vol. 256, no. 5, pp. 500–516, 2004.

[120] M. R. Thakare, J. A. Wharton, R. J. K. Wood, and C. Menger, "Exposure effects of alkaline drilling fluid on the microscale abrasion-corrosion of WC-based hardmetals," *Wear*, vol. 263, no. 1-6, pp. 125–136, 2007.

[121] B. T. Lu, J. F. Lu, and J. L. Luo, "Erosion-corrosion of carbon steel in simulated tailing slurries," *Corrosion Science*, vol. 53, no. 3, pp. 1000–1008, 2011.

[122] M. Abedini and H. M. Ghasemi, "Synergistic erosion-corrosion behavior of Al-brass alloy at various impingement angles," *Wear*, vol. 319, no. 1-2, pp. 49–55, 2014.

[123] J. O. Bello, R. J. K. Wood, and J. A. Wharton, "Synergistic effects of micro-abrasion-corrosion of UNS S30403, S31603 and S32760 stainless steels," *Wear*, vol. 263, no. 1-6, pp. 149–159, 2007.

[124] M. M. Stack, M. T. Mathew, and C. Hodge, "Micro-abrasion-corrosion interactions of Ni-Cr/WC based coatings: Approaches to construction of tribo-corrosion maps for the abrasion-corrosion synergism," *Electrochimica Acta*, vol. 56, no. 24, pp. 8249–8259, 2011.

[125] S. Akonko, D. Y. Li, and M. Ziomek-Moroz, "Effects of cathodic protection on corrosive wear of 304 stainless steel," *Tribology Letters*, vol. 18, no. 3, pp. 405–410, 2005.

[126] V. Sáenz de Viteri, G. Barandika, R. Bayón et al., "Development of Ti-C-N coatings with improved tribological behavior and antibacterial properties," *Journal of the Mechanical Behavior of Biomedical Materials*, vol. 55, pp. 75–86, 2015.

[127] F. B. Saada, Z. Antar, K. Elleuch, and P. Ponthiaux, "On the tribocorrosion behavior of 304L stainless steel in olive pomace/tap water filtrate," *Wear*, vol. 328-329, pp. 509–517, 2015.

[128] F. B. Saada, Z. Antar, K. Elleuch, P. Ponthiaux, and N. Gey, "The effect of nanocrystallized surface on the tribocorrosion behavior of 304L stainless steel," *Wear*, vol. 394-395, pp. 71–79, 2018.

[129] S. Mischler, S. Debaud, and D. Landolt, "Wear-accelerated corrosion of passive metals in tribocorrosion systems," *Journal of The Electrochemical Society*, vol. 145, no. 3, pp. 750–758, 1998.

[130] J. Jiang, M. M. Stack, and A. Neville, "Modelling the tribo-corrosion interaction in aqueous sliding conditions," *Tribology International*, vol. 35, no. 10, pp. 669–679, 2002.

[131] J. Jiang and M. M. Stack, "Modelling sliding wear: From dry to wet environments," *Wear*, vol. 261, no. 9, pp. 954–965, 2006.

[132] C. B. von der Ohe, R. Johnsen, and N. Espallargas, "Modeling the multi-degradation mechanisms of combined tribocorrosion interacting with static and cyclic loaded surfaces of passive metals exposed to seawater," *Wear*, vol. 269, no. 7-8, pp. 607–616, 2010.

[133] N. Papageorgiou and S. Mischler, "Electrochemical simulation of the current and potential response in sliding tribocorrosion," *Tribology Letters*, vol. 48, no. 3, pp. 271–283, 2012.

[134] S. Cao, S. Guadalupe Maldonado, and S. Mischler, "Tribo-corrosion of passive metals in the mixed lubrication regime: Theoretical model and application to metal-on-metal artificial hip joints," *Wear*, vol. 324-325, pp. 55–63, 2015.

[135] S. Guadalupe, S. Cao, M. Cantoni, W.-J. Chitty, C. Falcand, and S. Mischler, "Applicability of a recently proposed tribocorrosion model to CoCr alloys with different carbides content," *Wear*, vol. 376-377, pp. 203–211, 2017.

[136] S. Cao and S. Mischler, "Assessment of a recent tribocorrosion model for wear of metal-on-metal hip joints: Comparison between model predictions and simulator results," *Wear*, vol. 362-363, pp. 170–178, 2016.

[137] A. Dalmau, A. R. Buch, A. Rovira, J. Navarro-Laboulais, and A. I. Muñoz, "Wear model for describing the time dependence of the material degradation mechanisms of the AISI 316L in a NaCl solution," *Wear*, vol. 394-395, pp. 166–175, 2018.

[138] A. López, R. Bayón, F. Pagano et al., "Tribocorrosion behaviour of mooring high strength low alloy steels in synthetic seawater," *Wear*, vol. 338-339, pp. 1–10, 2015.

[139] A. López-Ortega, R. Bayón, J. Arana, A. Arredondo, and A. Igartua, "Influence of temperature on the corrosion and tribocorrosion behaviour of High-Strength Low-Alloy steels used in offshore applications," *Tribology International*, vol. 121, pp. 341–352, 2018.